Reconstructing historic Glacial Lake Outburst Floods through numerical modelling and geomorphological assessment

Westoby, Matthew John; Glasser, Neil Franklin; Hambrey, Michael John; Brasington, James; Reynolds, John M.; Hassan, Mohamed A. A. M.

Published in:
Earth Surface Processes and Landforms

DOI:
10.1002/esp.3617

Publication date:
2014

Citation for published version (APA):
Westoby, M. J., Glasser, N. F., Hambrey, M. J., Brasington, J., Reynolds, J. M., & Hassan, M. A. A. M. (2014). Reconstructing historic Glacial Lake Outburst Floods through numerical modelling and geomorphological assessment: Extreme events in the Himalaya. *Earth Surface Processes and Landforms*, *39*(12), 1675-1692. https://doi.org/10.1002/esp.3617

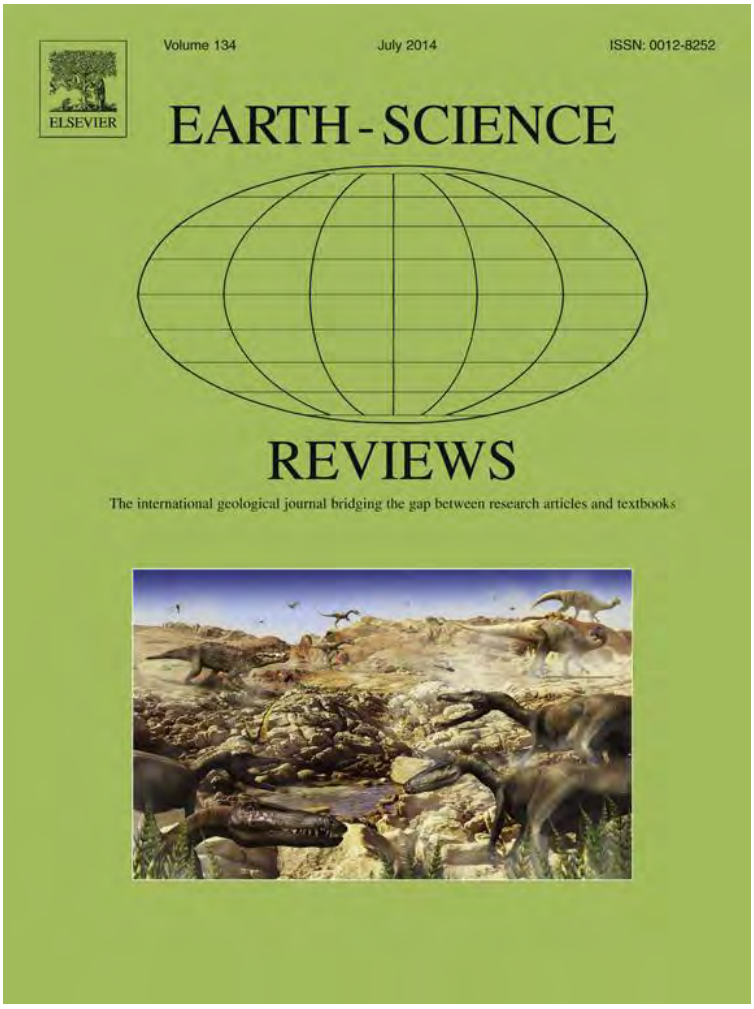

Earth-Science Reviews 134 (2014) 137–159

Contents lists available at ScienceDirect

Earth-Science Reviews

journal homepage: www.elsevier.com/locate/earscirev

Modelling outburst floods from moraine-dammed glacial lakes

M.J. Westoby [a,*], N.F. Glasser [a], J. Brasington [b], M.J. Hambrey [a], D.J. Quincey [c], J.M. Reynolds [d]

[a] Department of Geography and Earth Sciences, Aberystwyth University, Aberystwyth, SY23 3DB, UK
[b] School of Geography, Queen Mary, University of London, London, E1 4NS, UK
[c] School of Geography, University of Leeds, Leeds, LS2 9JT, UK
[d] Reynolds International Ltd, Suite 2 Broncoed House, Broncoed Business Park, Mold, CH7 1HP, UK

ARTICLE INFO

Article history:
Received 17 March 2013
Accepted 23 March 2014
Available online 3 April 2014

Keywords:
Glacial Lake Outburst Flood (GLOF)
Moraine dam
Dam-breach modelling
Hydrodynamic modelling

ABSTRACT

In response to climatic change, the size and number of moraine-dammed supraglacial and proglacial lake systems have increased dramatically in recent decades. Given an appropriate trigger, the natural moraine dams that impound these proglacial lakes are breached, producing catastrophic Glacial Lake Outburst Floods (GLOFs). These floods are highly complex phenomena, with flood characteristics controlled, in the first instance, by the style of breach formation. Downstream, GLOFs typically exhibit transient, often non-Newtonian fluid dynamics as a result of high rates of sediment entrainment from the dam structure and channel boundaries. Combined, these characteristics introduce numerous modelling challenges. In this review, the historical, contemporary and emerging approaches available to model the individual stages, or components, of a GLOF event are introduced and discussed.

A number of methods exist to model the stages of a GLOF event. Dam-breach models can be categorised as being empirical, analytical or numerical in nature, with each method having significant advantages and shortcomings. Empirical relationships that produce estimates of peak discharge and time to peak are straightforward to implement, but the applicability of these models is often limited by the nature of the case study data from which they are derived. Furthermore, empirical models neglect the inclusion of basic hydraulic principles that describe the mechanics of breach formation. Analytical or parametric models simulate breach development using simplified versions of the physically based equations that describe breach enlargement, whilst complex, physically-based codes represent the state-of-the-art in numerical dam-breach modelling. To date, few of the latter have been applied to investigate the moraine-dam failure problem.

Despite significant advances in the physical complexity and availability of higher-order hydrodynamic solvers, the majority of published accounts that have attempted to reconstruct or predict GLOF characteristics have been limited, often by necessity, to the use of relatively simplistic models. This is in part attributable to the unavailability of terrain models of many high-mountain catchments at the fine spatial resolutions required for the effective application of numerically-sophisticated codes, and their proprietary (and often cost-prohibitive) nature. However, advanced models are experiencing increasing use in the glacial hazards literature. In particular, the suitability of emerging mesh-free, particle-based methods for simulating dam-breach and GLOF routing may represent a solution to many of the challenges associated with modelling this complex phenomenon.

Sources of uncertainty in the GLOF modelling chain have been identified by various workers. However, to date their significance for the robustness of reconstructive and predictive modelling efforts have been largely unexplored and quantified in detail. These sources include the geometric and material characterisation of moraine dam complexes, including lake bathymetry and the presence and extent of buried ice, initial conditions (freeboard, precise spillway dimensions), spatial discretisation of the down-valley domain, hydrodynamic model dimensionality and the dynamic coupling of successive components in the GLOF model cascade.

Contents

* Corresponding author.
E-mail address: mjwestoby@gmail.com (M.J. Westoby).

http://dx.doi.org/10.1016/j.earscirev.2014.03.009
0012-8252/

1. Introduction

The recession of many glaciers in response to climate warming has led to a dramatic increase in the size and number of moraine-dammed supraglacial and proglacial lake systems (e.g. Ageta et al., 2000; Sakai et al., 2000; Benn et al., 2001; Iwata et al., 2002; Komori, 2008; Röhl, 2008; Gardelle et al., 2001; Janský et al., 2009; Thompson et al., 2012a). In Peru alone, outburst floods from glacial sources caused ~32,000 deaths in the 20th century, as well as destroying vital economic infrastructure, settlements and valuable arable land (Table 1; Lliboutry et al., 1977a; Reynolds, 1992; Richardson and Reynolds, 2000a). In the Nepal Himalaya, it has been estimated that the costs associated with the destruction of a mature single hydropower installation by an outburst flood could exceed $500 million (Richardson and Reynolds, 2000a).

Glacial Lake Outburst Floods (GLOF) are extremely complex phenomena. Each is a distinctly unique event, the characteristics of which are determined by, among other things, the triggering mechanism(s), reservoir hypsometry, the geometry, composition and structural integrity of the moraine dam, as well as the topography and geology of the flood path (Fig. 1). In this review, our definition of a GLOF refers exclusively to sudden-onset outburst floods which arise from the failure of a moraine-dam (Richardson and Reynolds, 2000; Table 1). This contrasts with other glacially sourced outburst floods, such as those resulting from the failure of an ice dam (e.g. Walder and Costa, 1996; Tweed and Russell, 1999; Roberts et al., 2003), volcanically triggered 'jökulhlaups' (e.g. Carrivick et al., 2004; Russell et al., 2010; Dunning et al., 2013), or the sudden release of water from englacial or subglacial reservoirs (Korup and Tweed, 2007).

A GLOF typically requires a trigger event. Triggers include ice and/or rock avalanches (e.g. Vuichard and Zimmerman, 1986; Evans, 1987; Costa and Schuster, 1988; Clague and Evans, 1994; Hubbard et al., 2005) or calving from the terminal face of a lake-terminating glacier (e.g. Lliboutry et al., 1977a; Blown and Church, 1985) which cause a displacement or seiche wave that has the capacity to overtop the dam-crest and initiate its failure. Additional triggers include the rapid input of glacial meltwater as a result of the sudden release of an englacial or subglacial reservoir (Clague and Evans, 2000; Richardson and Reynolds, 2000a,b), atmospheric triggers such as a high-intensity rainstorm or snowmelt event associated with a period of increased air temperatures (Korup and Tweed, 2007; Janský et al., 2010; Worni et al., 2012), or an earthquake that causes dam settlement or partial or full mechanical failure of the moraine dam (e.g. Osti et al., 2011).

In many cases, the rapid input of large volumes of material results in the displacement of lake water and subsequent overtopping of the dam structure, initiating breach formation (Richardson and Reynolds, 2000a; Balmforth et al., 2008). The degradation of a massive ice-core or permafrost may lower the dam crest and reduce freeboard, resulting directly in overspill and breach development, or reducing the minimum wave amplitude required to overtop the dam. Alternatively, an increase in lake volume, either suddenly, from a discrete rainfall or snowmelt event or the sudden release of water from an englacial or subglacial reservoir, or gradually, through a prolonged period of precipitation (e.g. Worni et al., 2012) may also trigger failure.

Breach formation is often manifested as the progressive erosion and enlargement of an incipient channel in the downstream face of the dam (e.g. Balmforth et al., 2008; Xu and Zhang, 2009). Eventually, the dam is

Table 1
Case study examples of different types of outburst floods from glacial sources.

Outburst type	Example	Description	References
Glacial Lake Outburst Flood (GLOF)	Dig Tsho, 1985 (Nepal Himalaya)	Failure triggered by overtopping from ice avalanche-triggered displacement waves. Reconstructed peak discharges of >2000 $m^3 s^{-1}$. Five fatalities, hydroelectric power station destroyed.	Vuichard and Zimmerman (1987), Cenderelli and Wohl (2001), Richardson and Reynolds (2000a)
	Sabai Tsho, 1998 (Nepal Himalaya)	Moraine destabilisation and failure believed to have been triggered by earthquake. Reconstructed GLOF peak discharge of 10,000 $m^3 s^{-1}$. 4.4 × 10^5 m^3 of sediment deposited within 14 km of breach.	Osti and Egashira (2009), Osti et al. (2011)
	Luggye Tsho, 1994 (Bhutan Himalaya).	Partial drainage of glacial lake, ~48 × 10^6 m^3 of water drained into the Pho Chhu river, producing a flood wave >2 m high 200 km from the source lake. 23 fatalities and widespread damage to buildings up to 84 km downstream.	Watanabe and Rothacher (1994), Richardson and Reynolds (2000b)
	Queen Bess Lake, 1997 (British Columbia)	Moraine dam overtopped by ice avalanche-triggered displacement wave. 8 × 10^6 m^3 water released. Peak discharges >1000 $m^3 s^{-1}$. Elevated water stage noticeable >100 km from source.	Clague and Evans (2000), Kershaw et al. (2005)
Glacier outburst (Jökulhlaup)	Grímsvötn lake, 1996 (Vatnajökull, Iceland)	Largest documented Icelandic jökulhlaup. Triggered by subglacial eruption. Peak discharges 4 × 10^4 $m^3 s^{-1}$, total volume of water released 3.2 km^2.	Guðmundsson et al. (1995), Russell et al. (1997), Björnsson (2002)
	Kverkfjöll, Holocene (Vatnajökull, Iceland)	Source of some of the largest Icelandic Holocene jokulhlaups. Reconstructed peak discharges of 0.5–10 × 10^4 $m^3 s^{-1}$. Fluvial erosion of bedrock and geomorphic work comparable to late Pleistocene 'megafloods'.	Carrivick (2007), Carrivick et al. (2004)
Glacier-dammed lake outburst	Indus and Yarkand rivers, (Karakoram Himalaya)	Numerous examples of glacier advance and damming of headwater rivers. Peak discharges believed to exceed 10^5 $m^3 s^{-1}$, causing significant erosion, sedimentation and secondary slope failure.	Hewitt (1982), Hewitt and Liu (2010).
	S. Tahoma Glacier, 1967– (Mt. Rainier, WA, USA)	Frequent outbursts recorded since 1967. Damage to infrastructure.	Walder and Driedger (1994)
	Altai Mountains (~13 ka BP) (Souther Siberia)	Quaternary ice-dammed lake outbursts producing 'megafloods' with maximum discharges of 10–18 × 10^6 $m^3 s^{-1}$. Last outburst believed to have occurred ~13 ka BP; peak discharge > 1 × 10^6 $m^3 s^{-1}$.	Rudoy (2002), Carling et al. (2009)
	Hubbard Glacier, 1986, 2002, (Alaska, USA.)	Glacier temporarily blocked entrance to Russell Fjord twice in recent history. In 1986, catastrophic failure of ice dam resulted in the release of ~5.4 km^3 of water, with peak discharges of up to 1 × 10^5 $m^3 s^{-1}$.	Mayo (1989), Motyka and Truffer (2007), Ritchie et al. (2008)

compromised, and water is released through the newly-formed outflow channel. Depending on factors including the cohesiveness of the dam material, breaching may be rapid, or more prolonged, and will result in either the partial or full breaching of the dam structure. The ultimate outcome is the downstream propagation of an outburst flood wave, which may take the form of a 'clearwater' low-viscosity flow, or, as has been more commonly documented, a high-viscosity, hyper-concentrated (sediment comprising ~20% of flow volume) or debris flow arising from the entrainment of vast quantities of debris sourced from the eroded dam structure and unconsolidated channel and flood-plain material (e.g. Lliboutry et al., 1977a; Blown and Church, 1985; Clague et al., 1985; Vuichard and Zimmerman, 1987; Clague and Evans, 2000; O'Connor et al., 2001; Kershaw et al., 2005).

Our understanding of the conditioning factors required for lake development and expansion has advanced considerably in recent decades, and can be largely attributed to advances in the capabilities of space-borne sensor technology and Geographic Information Systems (GIS) (e.g. Wessels et al., 2002; Quincey et al., 2005, 2007; Bolch et al., 2008), combined with field-based investigations of the morphology, sedimentology and internal structure of contemporary dams using ground-penetrating radar, self-potential or resistivity techniques (e.g. Pant and Reynolds, 2000; Richardson and Reynolds, 2000a,b; Haeberli

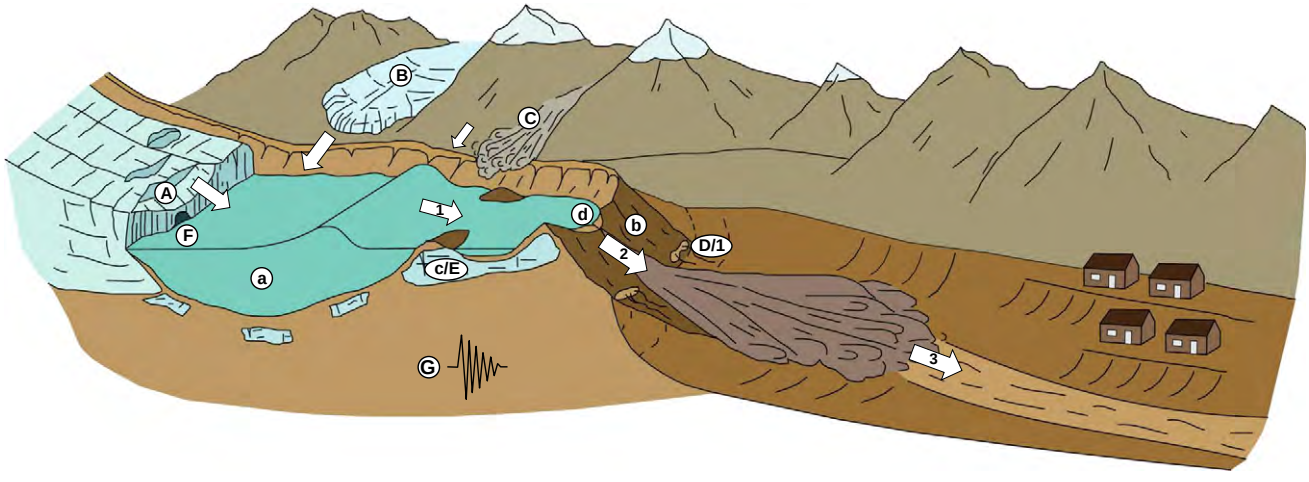

Fig. 1. Schematic of a hazardous moraine-dammed glacial lake. Potential triggers, conditioning factors, and key 'phases' in a GLOF event are highlighted. Potential triggers include: (A) contact glacier calving; (B) icefall from hanging glaciers; (C) rock/ice/snow avalanches; (D) dam settlement and/or piping; (E) ice-cored moraine degradation; (F) rapid input of water from supra-, en-, or subglacial (including subaqueous) sources; (G) seismicity Conditioning factors for dam failure include (a) large lake volume; (b) low width-to-height dam ratio; (c) degradation of buried ice in the moraine structure; (d) limited dam freeboard. Key stages of a GLOF include (1) propagation of displacement or *seiche* waves in the lake, and/or piping through the dam; (2) breach initiation and breach formation; (3) propagation of resultant flood wave(s) down-valley.
Adapted from Richardson and Reynolds (2000a)

et al., 2001; Reynolds, 2006; Hambrey et al., 2009; Langston et al., 2011; Moore et al., 2011; Reynolds, 2011; Thompson et al., 2012a,b) (Fig. 2), and surveys of expanding supraglacial lake systems (Benn et al., 2000; Richardson and Reynolds, 2000b; Benn et al., 2001; Thompson et al., 2012a) (Fig. 3).

This review considers the various modelling approaches that have been used for the reconstruction of palaeoGLOF (historical, typically ungauged) dynamics, and the prediction of potential future GLOF events. We first provide a detailed overview of the hazard, before considering hazard assessment of the lake basin and the modelling of potential triggering mechanisms. Dam overtopping and breach initiation and growth are then considered, before available hydrodynamic modelling approaches are introduced and discussed. The review concludes with a discussion of the advantages and limitations of various models and modelling approaches, including the identification of key areas for future research.

2. Moraine-dammed lakes

2.1. Neoglacial moraine dams

Moraine-dammed glacial lakes are found in the majority of alpine and high-mountain regions, with concentrations in the Andes (e.g. Lliboutry et al., 1977a; Reynolds, 1992; Emmer and Vilímek, 2013), the Hindu–Kush–Himalaya (HKH) arc (e.g. Richardson and Reynolds, 2000a; Mool et al., 2001; Komori, 2008; Bajracharya and Mool, 2009), the Tien Shan (Janský et al., 2010) and western Cordillera of North America (e.g. Clague and Evans, 1994; Evans and Clague, 1994; Clague and Evans, 2000; Kershaw et al., 2005). The majority of lateral and terminal moraine complexes, which impound present-day proglacial lakes were constructed during the 'Little Ice Age'; a globally-synchronous period of glacial advance extending from the 15th century to the end of the 19th century (Grove, 2004).

The main factors dictating the type of moraine dam that exists at a particular location are the longitudinal elevation profile of the parent glacier, or glaciers, and the availability of debris for supraglacial, englacial, or subglacial transport. Short, steep glaciers will respond to mass balance variations by advancing and retreating considerable distances. In contrast, long valley glaciers with shallow longitudinal profiles will respond to changes in mass balance by thickening and thinning, while the snout position remains relatively stable (Richardson and Reynolds, 2000a). Large, wide moraines thus tend to be associated with the latter glacier style, with steep, dynamic glaciers often lacking any significant terminal ridge at all. The mobilisation of supraglacial debris onto the former subglacial surface will result in the formation of 'dump' moraines (Benn and Owen, 2002). Most moraine-dams possess steep proximal and distal slopes, which may exceed angles of 40°, are typically devoid of any substantial vegetation cover, and are composed of poorly consolidated, unsorted, and uncohesive sediment (Costa and Schuster, 1988) (Fig. 4). Width-to-height ratios are controlled by the volume of material delivered to the glacier snout through the pathways mentioned above, and the length of time the terminus location remains stationary.

2.2. Lake formation

Provided the moraine is sufficiently consolidated and stable, glacial meltwater will pond in the deglaciated basin between the glacier terminus and moraine. This development pathway typically requires the presence of an overdeepened glacier bed (Frey et al., 2010). In the absence of a glacial overdeepening, the ponding of glacial meltwater may not be effective enough to produce a fully formed moraine-dammed lake. Depending on the permeability of the moraine, the lake will either continue to increase in volume until overtopping or piping occurs, or its volume will be naturally regulated as water seeps through the structure or over the dam crest (e.g. Lliboutry et al., 1977a; Costa and Schuster, 1988; Rana et al., 2000; Hubbard et al., 2005). In the case of the latter, a stable drainage regime will persist indefinitely if flow discharge is unable to entrain the coarser fraction of morainic material, resulting in natural armouring of the outflow channel (Costa and Schuster, 1988).

Alternatively, in situ glacier downwasting may result from the presence of inverted ablation gradients in the lower reaches as a result of downglacier increases in surface debris cover. This leads to a decrease in driving stresses and glacier velocity and causes, in turn, glacier stagnation (Benn et al., 2001, 2012). This, in turn, promotes the development of supraglacial ponds which, if drainage through englacial or supraglacial conduits is avoided, may coalesce to form a 'proto' moraine-dammed lake (Hochstein et al., 1995; Reynolds, 2000; Sakai et al., 2000; Benn et al., 2001; Wessels et al., 2002; Röhl, 2008; Sakai et al., 2009; Sakai and Fujita, 2010; Benn et al., 2012; Thompson et al., 2012a) (Fig. 3). Lakes that have originated in this way are particularly associated with debris-covered glaciers (Benn et al., 2000; Reynolds, 2000; Benn et al., 2001; Thompson et al., 2012a), as the irregular surface topography and typically low surface gradients of the glacier tongue are conducive to supraglacial lake formation (Reynolds, 1981, 2000; Quincey et al., 2007). Geometrically, moraines that have developed from the surface lowering of glacier tongues with thick supraglacial debris are typically large, complicated complexes with steep outwash fans (see geomorphological and sedimentological analyses in Hambrey et al., 2009, and Benn and Owen, 2002), whereas moraines and outwash fans formed by comparatively 'clean' glaciers are somewhat more subdued (Benn and Owen, 2002).

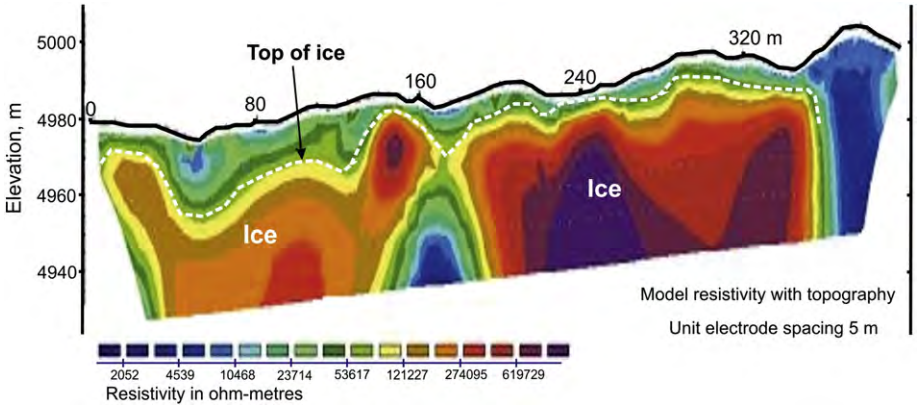

Fig. 2. Electrical resistivity profile along a transect across the terminal moraine complex of Imja Glacier, Khumbu Himal, Nepal, revealing the presence of buried ice (modified from fig. 7c, Reynolds, 2006).

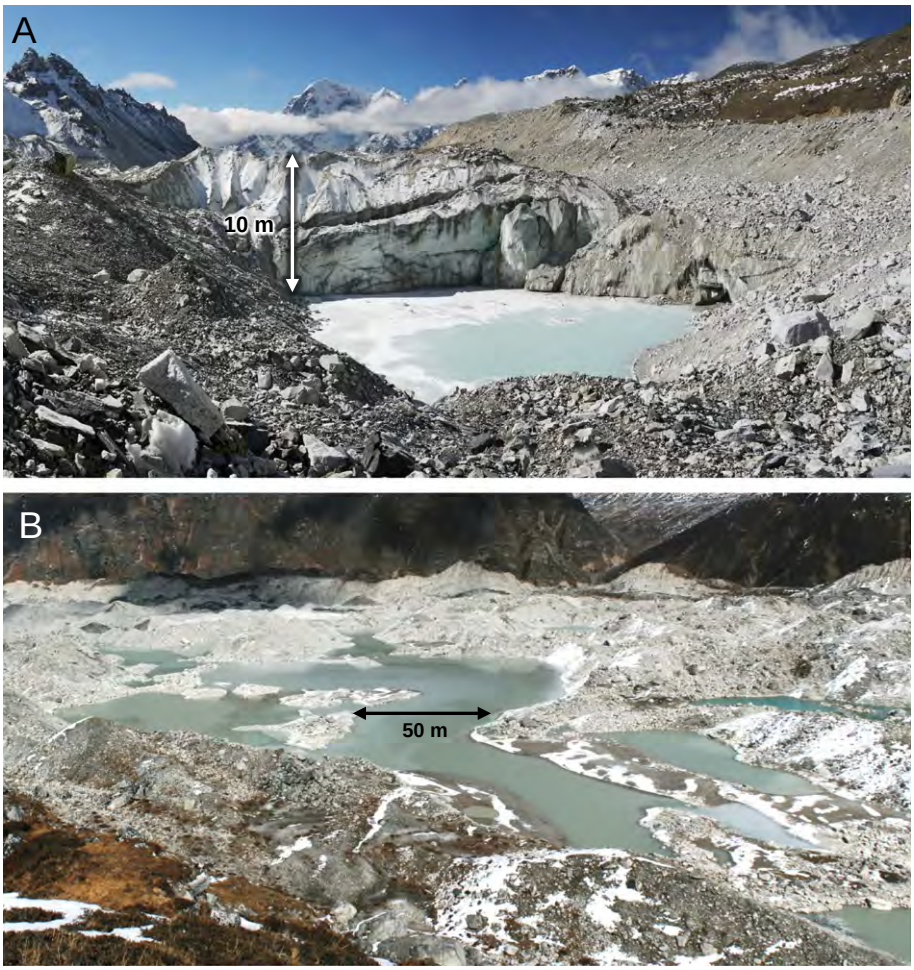

Fig. 3. The temporal evolution of supraglacial ponds on Ngozumpa Glacier, Khumbu Himal, Nepal; (A) supraglacial pond with calving ice face; (B) coalesced melt ponds and subsequent development of a 'proto' glacial lake.

2.3. Trigger mechanism

Many documented GLOFs have been initiated by overtopping waves caused by external triggers (e.g. Lliboutry et al., 1977a; Clague and Evans, 2000; Richardson and Reynolds, 2000a; Kershaw et al., 2005). Triggers include (often combined) ice and rock avalanches or landslides (e.g. Vuichard and Zimmerman, 1987; Harrison et al., 2006), or discrete glacier calving events (both sub-aerial and sub-aqueous) (e.g. Lliboutry et al., 1977a; Blown and Church, 1985). Additional triggers include dam settlement, piping, and lateral moraine collapse as a result of seismic activity (e.g. Osti et al., 2011), temporary blockage of an overflow channel (e.g. Huggel et al., 2004; Mergili and Schneider, 2011) or the flotation of submerged dead ice, resulting in water displacement (Richardson and Reynolds, 2000b). A number of conditioning factors may also predispose a particular moraine dam to fail, such as low freeboard, a high height-to-width dam ratio (Huggel et al., 2002a; McKillop and Clague, 2007; Quincey et al., 2007; Emmer and Vilímek, 2013), and sedimentological and structural characteristics (e.g. loosely consolidated, saturated sediment), as well as the presence of degrading permafrost or a massive buried ice core (Watanabe et al., 1995; Richardson and Reynolds, 2000b) (Fig. 2). A consideration of approaches to model the various triggers is presented in Section 3.1.

3. Approaches to modelling

A number of methods can be used to model the various stages or 'components' of a GLOF (Fig. 1), either empirically, analytically, or numerically. We classify these components according to their physical location and temporality in the GLOF modelling cascade, and define them as follows:

1. Trigger mechanism
2. Breach initiation and development
3. Downstream routing of the outburst flood wave(s)

3.1. Trigger mechanism

3.1.1. Ice, snow, and rock avalanching

The increasing capability of Geographic Information Systems (GIS), coupled with the wide availability and affordability of multi-temporal imagery and topographic data products from space- and airborne platforms has facilitated the production of largely desk-based natural hazard assessments (e.g. Huggel et al., 2002a, 2004; Salzmann et al., 2004; Kääb et al., 2002, 2005; Quincey et al., 2005; Huggel et al., 2005; McKillop and Clague, 2007; Allen et al., 2008). Potential triggering events, such as avalanche or landslide starting zones in close proximity to glacial lakes, can be identified using a relatively straightforward procedures including spectral band segmentation, thresholding, and DEM-derived slope classification, in combination with detailed aerial photography or high-resolution satellite imagery (Margreth and Funk, 1999; Salzmann et al., 2004; Quincey et al., 2005; Huggel et al., 2006; Allen et al., 2008).

The identification of potentially dangerous glaciers or rock slopes, followed by the mapping of potential avalanche run-out tracks, and

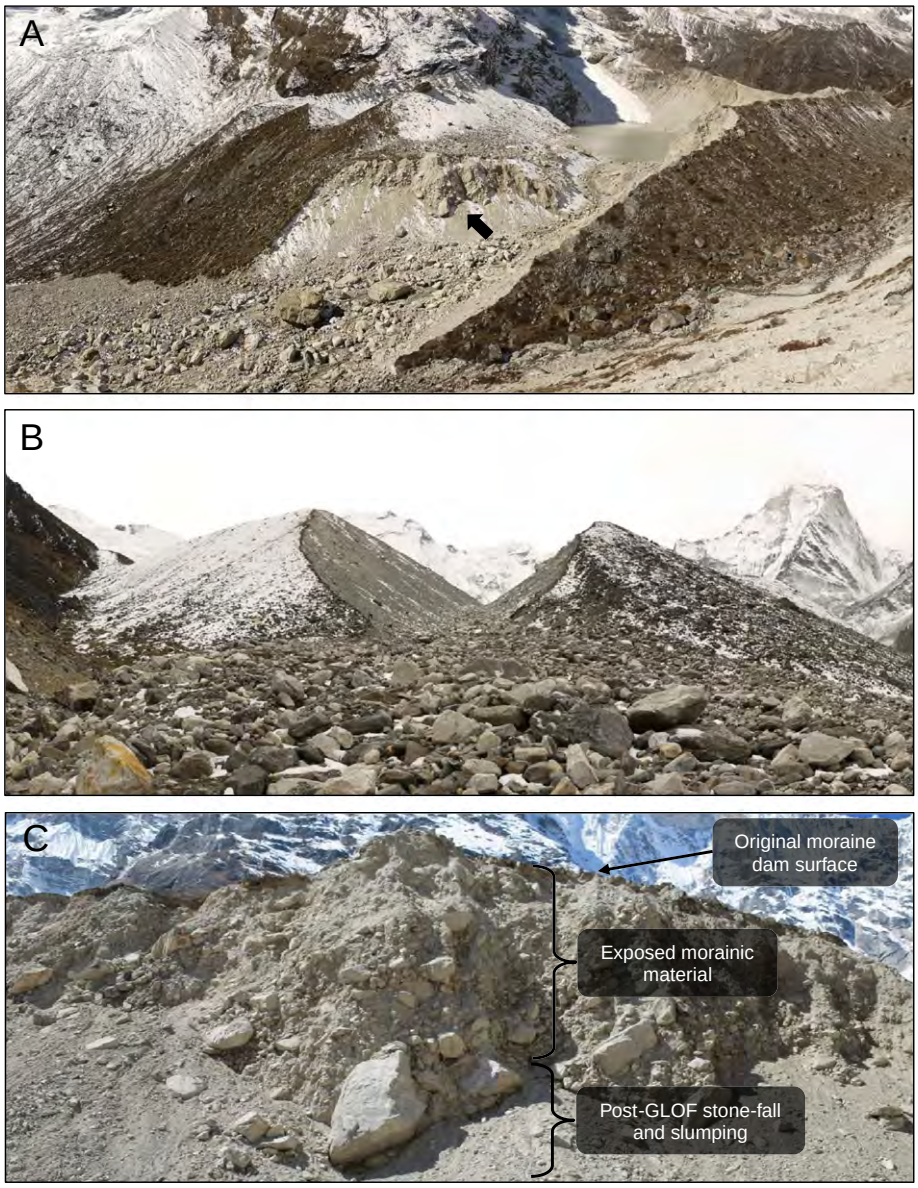

Fig. 4. Breached moraine dams in the Khumbu Himal, Nepal: (A) Dig Tsho. An ice avalanche, originating from the hanging remnants of Langmoche Glacier, entered the lake. Displacement wave(s) subsequently overtopped the terminal moraine (Vuichard and Zimmerman, 1987). A sizeable breach (centre, foreground) was formed by the escaping floodwaters. Black arrow indicates area shown in C; (B) Chukhung Glacier terminal moraine. For scale, maximum breach top width is ~90 m. Little is known about the dam failure dynamics of this GLOF, although it is estimated that approximately 5.5×10^5 m^3 of water was impounded before failure, based on reconstructed pre-GLOF dam and lake geometry (M Westoby, unpublished data); (C) Panoramic photograph of exposed sediment in the central section of a moraine dam breach, Dig Tsho, Nepal. Widespread, post-GLOF deposits are present at the base of the exposure. In this example, large boulder- and cobble-sized clasts are supported in a poorly-sorted, unconsolidated sand-gravel matrix. Total section is 150 m in length and 11 m high at the point of annotation.

the identification of potentially hazardous process combinations, such as an avalanche or landslide entering a glacial lake can then form the basis for more detailed investigation (Salzmann et al., 2004). The identification of subtle features such as bedrock tension cracks and jointing or overhanging glacial seracs which may provide clues as to the location of potential rock or ice avalanche starting zones remains challenging, particularly in the absence of very fine-resolution spaceborne or airborne imagery for many areas of interest (e.g. Huggel et al., 2006). GIS-based identification of contemporary or, in light of climate warming, potential future avalanche or landslide starting zones (see, e.g. Frey et al., 2010) remains the most viable approach. Mass movement trajectory modelling based on statistical parameters (e.g. Alean, 1985; Huggel et al., 2004) one-dimensional centre-of-mass models (e.g. Mergili et al., 2012), or more advanced physically based distributed models (e.g. Hungr, 1995; Sampl and Zwinger, 2004) may be used to predict plausible avalanche run-out distances and inundation areas, although advanced two- and three-dimensional models based on computational fluid dynamic (CFD) theory are required if dynamic behaviour such as deformation and lateral spreading of the avalanche or landslide body are to be realistically simulated (e.g. Sampl and Zwinger, 2004; Sailer et al., 2008). Progress in our understanding of the dynamics of rock-ice avalanches has been made in recent years by workers including Schneider et al. (2010), who used a two-dimensional numerical model, RAMMS (Christen et al., 2010), in combination with seismic data recordings to infer a proportional relationship between the latter and the frictional work rate of an avalanche.

3.1.2. Glacier calving

Prediction of calving rates, or more importantly for hazard assessment, the prediction of volumes of discrete calving events and

characteristics of triggered impulse waves is far from straightforward. Progress in understanding the glaciological (e.g. Benn et al., 2007) and limnological factors governing thermo-erosional notch development (e.g. Röhl, 2006) has improved in recent years, and has provided insights into the prediction of future calving rates under future warming scenarios. Long-term monitoring of calving frequency, including impulse wave heights, may aid prediction of the likely occurrence of waves capable of overtopping terminal moraine structures. Alternatively, an artificial reduction in dam freeboard through manual intervention, specifically lake level lowering (e.g. Grabs and Hanisch, 1993), has been carried out at sites in the Peruvian Andes (e.g. Lliboutry et al., 1977a; Reynolds, 1992, 1998a,b; Reynolds et al., 1998) and Nepal Himalaya (e.g. Reynolds, 1998a,b; Yamada, 1998). As well as reducing hydrostatic pressure in the moraine dam complex, this also serves to increase the minimum wave amplitude required for overtopping, though at the risk of increasing calving activity via decreased ice-tongue support by buoyancy forces, with potentially disastrous consequences (Lliboutry et al., 1977a).

3.1.3. Wave overtopping

Many documented moraine dam failures have been initiated by overtopping by waves generated from landslides or ice avalanches (e.g. Lliboutry et al., 1977a; Costa and Schuster, 1988; Clague and Evans, 2000; Richardson and Reynolds, 2000a). Numerous moraine dams, both failed and intact, show evidence of overtopping by displacement waves (Lliboutry et al., 1977a,b; Blown and Church, 1985; Costa and Schuster, 1988; Clague and Evans, 2000; Richardson and Reynolds, 2000a; Hubbard et al., 2005; Kershaw et al., 2005). Whilst these waves might not technically be a trigger for moraine-dam failure in their own right, as a preceding initiation mechanism must have occurred, it is often the erosive power of their run-up and passage across a moraine-dam that may initiate its failure.

Waves generated by sub-aerial mass flows such as landslides or avalanches fall into one of two categories. The first is a solitary displacement wave formed by the 'pushing' of the top level of the water column. The second is classified as a standing wave, or 'seiche', formed when the volume and entry velocity of the external mass is large enough to trigger the mobilisation of the entire water column (Fig. 5). Resultant 'sloshing' of the water in the enclosed moraine basin causes the repeated run-up of water at the lake boundaries and may be highly effective at eroding the dam structure (e.g. Hubbard et al., 2005; Balmforth et al., 2008). Based on geomorphological evidence, Hubbard et al. (2005) undertook a comprehensive reconstruction of seiche dynamics in a moraine-dammed glacial lake in Peru. On 22 April 2002 a rock avalanche deposited 8–20 $\times$ 10^6 m^3 of material onto the surface of the terminus of Glaciar Pucajirca, ~5 $\times$ 10^6 m^3 of which directly entered moraine-dammed Laguna Safuna Alta and triggered a seiche. The lake had been artificially lowered prior to the event, though still posed a potential failure risk. The initial overtopping wave height is estimated to have exceeded 100 m. The presence of multiple erosion discontinuities on the proximal face of the latero-terminal moraine complex suggests that at least ten seiche waves reached the moraine dam, with at least one wave becoming entirely airborne. Whether more than one wave overtopped the dam structure is unknown. Following two failures in 1951 (Reynolds, 1992), evidence of multiple wave run-ups was also observed by Lliboutry et al. (1977a) at Artesoncocha, another Peruvian moraine-dammed lake.

The dimensions and propagation rate of a displacement wave are determined by the mass, geometry, velocity (both subaerial and subaqueous), and angle of entry of material into a standing body of water, as well as the lake area and bathymetry (e.g. Fritz et al., 2003a; Walder et al., 2003). For obvious reasons, empirical equations to represent impulse wave characteristics have been derived almost exclusively from physical scale, laboratory-based experiments (e.g. Fritz et al., 2003a,b; Walder et al., 2003; Ataie-Ashtiani and Nik-Khah, 2008; Balmforth et al., 2008, 2009). As a result, such experiments are typically not able to simulate the effects of, for example, observed, complex basin bathymetry on wave propagation and run-up (Synolakis, 1987). Few studies also appear to have taken into consideration the effects of lateral spreading where the source of the landslide or avalanche is the valley flanks (e.g. Risley et al., 2006), though such problems may be overcome by the use of numerical flow models (e.g. Cannata et al., 2012).

From a hazard development perspective, the interaction of a displacement wave, or a series of seiche waves with the moraine dam structure is important. Required, therefore, are estimates of overtopped water volumes and inundation depths with which to force breach erosion and flood-routing models. Of note are recent scaled experiments conducted by Balmforth et al. (2008, 2009), who used a combination of physical and theoretical modelling to assess the impact of large displacement waves on moraine dam structures. Their results demonstrated that initiation of the breaching process ultimately amounts to a competition between erosion and rates of lake drainage and seiche damping. A threshold was identified whereby the amplitude of the initial wave, or rate of erosion, should exceed a critical value for catastrophic dam failure to be initiated (Balmforth et al., 2009).

3.1.4. Atmospheric triggers

Heavy precipitation (e.g. Worni et al., 2012) or a glacial outburst flood from an adjacent ice mass may trigger a rapid increase in lake volume and level and the subsequent enlargement and down-cutting of an

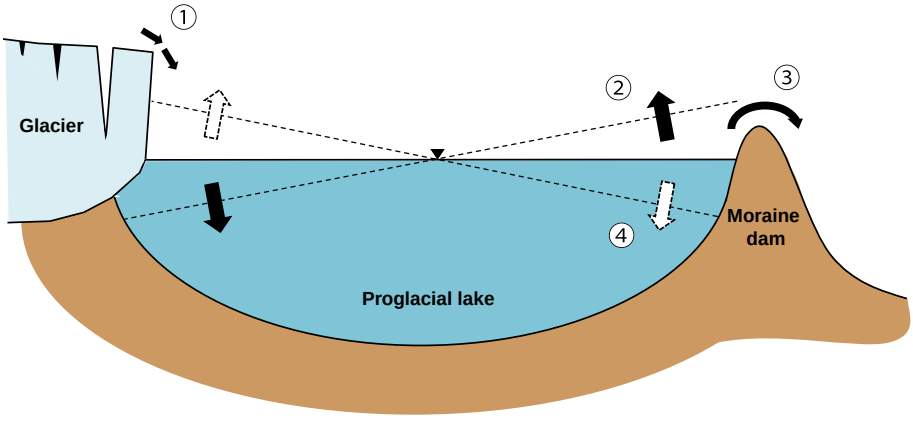

Fig. 5. Dynamics of a standing wave or 'seiche': (1) input of external mass to the lake system (e.g. a large glacier calving event); (2) mobilisation of the entire water column, and; (3) subsequent overtopping of dam structure, followed by (4) continuing, but attenuating, oscillations of the water body, which may or may not result in further overtopping. Black triangle represents the water surface pivot point, around which the standing wave oscillates. Note: figure dimensions for illustrative purposes only and not necessarily to scale.

existing spillway, or the initiation of a new channel (Clague and Evans, 1992, 2000). Quantifying the minimum volume of water required to fill a lake is relatively straightforward if basin perimeter and freeboard are known and seasonal variations in water level are taken into account (e.g. Janský et al., 2010). However, it is difficult to predict the timing and volume of water released, particularly where historical outbursts from the glacier in question have not been documented.

3.1.5. Ice-cored moraine degradation

Modelling the degradation of ice-cored moraine complexes is challenging. Subsidence caused by the melting of interstitial ice or a massive ice core reduces the structural integrity of a dam, thereby increasing the propensity for failure (Richardson and Reynolds, 2000b). Consequently, dam freeboard is reduced through lowering of the dam crest, thereby reducing the minimum amplitude of displacement waves required to overtop the dam, or reducing the additional volume of glacially- or meteorologically-derived water required to fill the reservoir and overflow the dam. Quantification of moraine surface lowering has been achieved either by in situ monitoring (e.g. Reynolds, 1992; Watanabe et al., 1995; Pant and Reynolds, 2000; Janský et al., 2009), or the assessment of multi-temporal, high-resolution digital terrain models (DTMs) (cf. Irvine-Fynn et al., 2011; Bennett and Evans, 2012; Sawagaki et al., 2013). The disadvantage of the former is that it is typically extremely challenging from a logistical perspective, whilst DTM errors associated with the latter should not exceed the anticipated change in moraine surface elevation over the investigation timescale, which is often small.

3.1.6. Earthquake-triggered dam failure

Modelling the response of a glacier-moraine-dammed lake system to an earthquake (Dai et al., 2005; Strasser et al., 2008) is incredibly difficult, not least because of the unpredictability associated with estimating the timing and magnitude of a seismic event (and its seismic signature in the vicinity of a glacial lake, which may be hundreds of kilometres from the earthquake epicentre). Analysis of geological maps may help to identify whether an area that contains moraine-dammed lakes lies close to active faults, and is therefore at an elevated risk of experiencing earthquake-induced GLOFs. However, by their very nature, many mountain ranges are tectonically active, and so it might be argued that this trigger should be automatically considered as a trigger in the majority of cases. Detailed field investigation in support of geotechnical characterisation of a moraine-dam may provide an indication of its susceptibility to settlement and piping in the event of an earthquake, whilst semi-quantitative analysis of the structural characteristics of calving faces of lake-terminating glaciers from field investigation or remotely sensed imagery may aid prediction of the likelihood of mass failure and the estimation of displacement wave dimensions. However, this is far from an exact science.

3.2. Dam-breach

3.2.1. Breach initiation

Sudden or gradual overtopping and inundation, or internal failure as a result of piping and seepage may result in the development of a breach through the moraine dam (Fig. 4). In the case of the former, overtopping water is likely to traverse the width of the dam crest as a uniform sheet (e.g. Kershaw et al., 2005). Alternatively, flow through an existing outlet will be augmented (Costa and Schuster, 1988). Erosion of the dam will occur if the increased boundary shear stresses exerted by the overtopping or channelized flow exceed the cohesive strength of the surface material (Korup and Tweed, 2007). This permits increased discharge from the lake, which in turn may result in runaway incision. Incision will cease when one of the following occurs: i) the base-level of the moraine is reached; ii) a bedrock abutment (or a significant decrease in material erodibility) is encountered; or iii) the outflow channel becomes sufficiently armoured to halt down-cutting (e.g. Clague and Evans, 1992).

Breaches initiated by internal failure of the dam structure are considerably less well understood, although the underlying principle is that saturation and subsequent seepage of lake water through the dam structure causes the finer fraction of the sediment to be removed, forming 'pipes' and thereby reducing the local physical strength of the dam material (Clague and Evans, 2000; Korup and Tweed, 2007). In addition, thermokarst degradation of buried ice contained within the moraine structures has been observed (Richardson and Reynolds, 2000b). Collapse of subsurface cavities may lead to a lowering of dam crest elevation, thereby increasing the likelihood of an overtopping failure. The transition to open breach formation is initiated through slumping and mechanical failure and collapse of the overlying material.

The detailed simulation of breach formation processes is central to an assessment of the downstream hazards posed by a GLOF, since the shape of the breach hydrograph (Fig. 6, Table 2) will determine, in the first instance, the peak discharge at the flood source. This hydrograph will typically be used as an upstream boundary condition for subsequent flood routing. In order of increasing complexity, models used in published simulations of moraine dam failure events may be generally classed as one of the following: i) empirical regression models; ii) analytical and parametric models; iii) physically-based, numerical models.

3.2.2. Empirical dam-breach models

Empirical models represent the simplest approach to dam-break modelling (Table 3). These models are not process-based and comprise a single or series of regression relationships derived from test case studies or observed historical dam failures (e.g. Macdonald and Langridge-Monopolis, 1984; Blown and Church, 1985; Costa and Schuster, 1988; Froehlich, 1995; Wahl, 1998). Examples of empirical equations used for dam-break modelling are provided in Wahl (2004), who also undertook a comprehensive investigation of uncertainty estimates surrounding the use of such equations, and also Thornton et al. (2011). Input parameters typically include a combination of the following: dam width, height, lake area and volume. If unknown, lake volume may also be approximated using a separate empirically-derived equation (see e.g. Huggel et al., 2002a,b). Model output typically comprises a single discrete value, such as peak discharge (Q_p) (e.g. Hagen, 1982; Walder and O'Connor, 1997) or time to peak (T_p) (e.g. MacDonald and Langridge-Monopolis, 1984; Froehlich, 1995). Such models have been widely used in the glacial hazards literature. One of the earliest examples is presented by Clague and Mathews (1973), who discovered that the magnitude of the peak discharge of a glacial outburst flood arising from the failure of an ice-dammed lake is approximately proportional to the available volume of stored water. An applied example of the use of empirical models is provided by Vuichard and Zimmerman (1986, 1987), who applied the relationships of Hagen (1982), MacDonald and Langridge-Monopolis (1984), and Blown and Church (1985) to

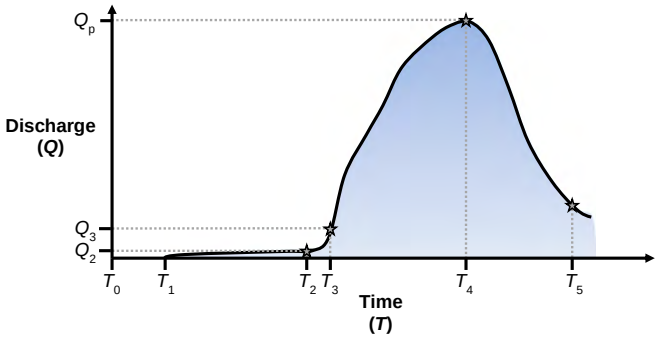

Fig. 6. Generic dam breach outflow hydrograph. Axis annotation is explained in Table 2. Modified from fig. 2.7, Morris et al. (2009).

Table 2
Description of phases comprising a generic dam breach outflow hydrograph (see Fig. 7) and qualitative description of our ability to model them. Adapted from Morris et al. (2009).

Time	Description	Modelling ability
T_0	No breach initiation	–
T_1	Start of breach initiation. Seepage over or through dam begins.	Limited
T_1–T_2	Breach initiation phase. Q typically low. May last hours–months (Q_2)	Poor
T_2–T_3	Critical transition to breach formation. Erosion reaches upstream face of dam, initiating rapid breach growth (Q_3)	Limited
T_3–T_5	Breach formation. Rapid vertical erosion dominates initially, followed by continued vertical and lateral erosion.	Poor–moderate
T_4	Peak discharge (Q_p)	Good

estimate the peak discharge (6–8000 m^3/s) of the 1985 Dig Tsho GLOF, Nepal.

However, such relations are limited in their suitability for predictive purposes, as they neglect the inclusion of basic hydraulic principles pertaining to breach initiation and enlargement and are typically derived from a range of failed dam types and settings, including artificial constructs (Walder and O'Connor, 1997). In their appraisal of pre-existing empirical relations, Walder and O'Connor (1997) maintained that such relationships were flawed in their assumption that Q_p may be simply approximated as the product of volume of water released and the resulting drop in lake level, instead recognizing that hydraulic principles and constraints, such as breach erosion rate, are equally as important. Though theoretically more robust than standard empirical equations, this approach assumes that the user is able to quantify breach erosion rates. The impracticalities of quantifying the physical processes at work during breach formation are numerous, and although experimental progress in this field has been made in recent years (e.g. Morris et al., 2007), in practice these parameters are generally unknown and extremely challenging to quantify in the field. Providing the geometric characteristics of the dam structure and attendant lake basin are known, empirical relations represent an expeditious and simple approach to estimating Q_p, and, at first glance, would appear suitable for relatively basic hazard assessment. Taking the above into account and without reliable estimates of time to peak flow and consideration of the form of rising and falling limbs of the outflow hydrograph, such data have limited value for the assembly of inundation maps and reach-specific hydrograph and flood attenuation data. However, whilst the derivation of individual hydrographs may be appropriate for reconstructive GLOF modelling efforts, where detailed process analysis and geomorphological inference might be applied to constrain model boundary conditions and input parameters, the merits of adopting a deterministic approach for predictive GLOF modelling is questionable given the inherent variability of material properties and model boundary conditions. We consider the extent and significance of uncertainty in the GLOF model chain in Section 5.

3.2.3. Analytical and parametric dam-breach models

Analytical and parametric models are semi-physically based, given their consideration of simplified physical processes (Morris et al., 2009b). These models incorporate simplified numerical treatments of the physical processes involved during the breach development phase (e.g. Capart, 2013), and typically assume that the rate of breach growth is purely time-dependent. Accordingly, the user is required to enter morphometric boundary conditions including final breach geometry (e.g. base width and side slope angle) and the time required for full formation. The model then proceeds to iteratively calculate the outflow hydrograph as the breach develops. Another assumption is that weir equations can be used to represent flow over the dam. Such equations typically assume the form:

$$Q = Cd\, L\, H^{\frac{3}{2}} \tag{1}$$

with:

$$H = h_w + \frac{V^2}{2g} \tag{2}$$

Table 3
Empirical equations used to estimate peak discharge (Q_p) for natural dam failures. Examples marked with an asterisk (*) have been derived entirely from case studies of moraine-dam failure.

Type	Reference	Type	R^2 (if known)	No. case studies		Empirical equation
				Real	Simulated	
Height of water equations	Kirkpatrick (1977)	Best fit	0.790	13	6	$Q_p = 1.268(H_w + 0.3)^{2.5}$
	US Soil Conservation (1981)	Envelope	–	13		$Q_p = 16.6(H_w)^{1.85}$
	US Bureau of Reclamation (1982)	Envelope	0.724	21		$Q_p = 19.1(H_w)^{1.85}$
	Singh and Snorrason (1982)	Best fit	0.488		8	$Q_p = 13.4(H_d)^{1.89}$
	* Walder and O'Connor (1997)	Best fit	0.620	9		$Q_p = 0.045(V)^{0.66}$
	Pierce et al. (2010)	Best fit	0.633	72		$Q_p = 0.784(H)^{2.668}$
		Best fit	0.640	72		$Q_p = 2.325\ln(H)^{6.405}$
Storage equations	Singh and Snorrason (1984)	Best fit	0.918		8	$Q_p = 1.776(V)^{0.47}$
	Evans (1986)	Best fit	0.836	29		$Q_p = 0.72(V)^{0.53}$
	* Walder and O'Connor (1997)	Best fit	0.090	9		$Q_p = 60.3(V)^{0.84}$
Height of water and storage equations	Hagen (1982)	Envelope	–	6		$Q_p = 0.54(V\,H_w)^{0.5}$
	Macdonald and Langridge-Monopolis (1984)	Best fit	0.788	23		$Q_p = 1.154(V\,H_w)^{0.412}$
		Envelope	0.156	23		$Q_p = 3.85(V_w H_w)^{0.411}$
	Costa (1985)	Best fit	0.745	31		$Q_p = 0.763(V\,H_w)^{0.42}$
	* Costa and Schuster (1988)	Best fit	0.780	8		$Q_p = 0.00013\ (PE)^{0.60}$
		Envelope	–			$Q_p = 0.063\ (PE)^{0.42}$
	Froehlich (1995)	Best fit	0.934	22		$Q_p = 0.607(V^{0.295}\,H_w^{1.24})$
	* Walder and O'Connor (1997)	Best fit	0.490	9		$Q_p = 0.19(H_w\,V)^{0.47}$
	Pierce et al. (2010)	Best fit	0.844	87		$Q_p = 0.0176(VH)^{0.606}$
		Best fit	0.850	87		$Q_p = 0.038(V^{0.475}H^{1.09})$
Other	Thornton et al. (2011)	Best fit	0.909	14		$Q_p = 0.1202(L)^{1.7856}$
		Best fit	0.871	25		$Q_p = 0.863(V^{0.335}H^{1.833}\,W_{av}^{-0.663})$
		Best fit	0.991	14		$Q_p = 0.012(V^{0.493}H^{1.205}L^{0.226})$

and:

$$V = \frac{Q_a}{A} \tag{3}$$

where Q is flow discharge ($m^3\ s^{-1}$), Cd is a weir coefficient, L is the width of the weir, h_w is the hydraulic head of the impounded water above the dam crest, V is the average velocity (m/s) of flow immediately upstream of the weir, Q_a is the actual flow rate, and A is the cross-sectional channel area (m^2). Cd can be determined by dividing Q_a by the theoretical flow rate, Q_t. Where one or more input parameters must be approximated, there exists an associated danger of over- or underestimation of dam-breach peak discharge or time to peak (or both), making sensitivity analyses of input parameter combinations an essential undertaking.

Early flood routing models developed by the United States National Weather Service (NWS), including DAMBRK (Fread, 1988a) and FLDWAV (Fread, 1993), utilise the parametric model BREACH (Fread, 1988b) to compute an upstream hydrograph. GLOF modelling studies that have adopted semi-physical breach models include Meon and Schwarz (1993), who used DAMBRK to reconstruct the 1981 GLOF from Zhangzanbo Lake, Nepal, and Shrestha et al. (2010), who used BOSS-DAMBRK (an enhanced version of the original DAMBRK model) to estimate patterns of flood inundation in the Sun Koshi basin, Nepal. Osti and Egashira (2009) used the NWS Simplified Dam Break (SMPDBK) model (see Whetmore et al., 1991), combined with an empirical predictor of failure duration (Froehlich, 1995) to reconstruct the 1998 GLOF from Sabai Tsho glacial lake in the Khumbu Himal, Nepal. Dam-breach modelling undertaken fails to account for dead ice and the heterogeneous nature of the moraine dam structure, and thereby precluding an accurate simulation of the moraine breaching process.

3.2.4. Fully physically based numerical models

Complex numerical models are based predominantly on the physical processes observed during failure, including breach flow hydraulics and sediment transport, as well as soil erodibility relationships and structural models to simulate breach widening (e.g. Mohamed et al., 2002; Worni et al., 2012). Purely numerical models have not seen widespread use in the dam-breach literature. This may be attributed in part to their comparatively high computational cost, although with the rapid advent of affordable, high-end desktop computers this should cease to be an issue in the near future. With respect to outbursts from moraine-dammed lakes, the most commonly used numerical models have been NWS DAMBRK (Carling and Glaister, 1987; Fread, 1988a) and BREACH (Fread, 1988b; O'Connor et al., 2001; Bajracharya et al., 2007; Xin et al., 2008; Shrestha et al., 2010), although the adoption of advanced models appears to be becoming more commonplace.

3.3. Glacial Lake Outburst Flood routing

Floods from sudden dam failures, often termed 'dam-break outburst floods', are characterised by the often short-lived passage of high-magnitude floodwaters and associated transient flow hydraulics (Marren, 2005; Carrivick, 2010). The rate and style of breach formation, which, in the first instance, determines breach hydrograph form (Fig. 6), exerts a dominant control on flood dynamics in the 'near field', or through immediate downstream reaches. However, with increasing distance from the flood source, valley characteristics including topography (e.g. channel slope, bends, and channel geometry), vegetation (e.g. Lancaster et al., 2003) and sediment availability play a more dominant role (Richardson and Reynolds, 2000a). Floods which entrain vast quantities of uncohesive sediment, sourced from the moraine dam and deposits on the valley floor and sides may become transformed into debris flows (Clague et al., 1985; Evans, 1986; Rickenmann, 1999; Clague and Evans, 2000). Such flows are capable of achieving far greater runout distances than typical clearwater flows, owing to the increased momentum afforded by the combination of fluid and solid forces (and resultant transition to a non-Newtonian flow regime) and continuing addition of material through bed and bank erosion (Iverson, 1997). However, evidence from historical GLOFs and debris flows suggests such flows are unlikely to form or be sustained on slopes of less than 10–15° (e.g. Clague and Evans, 1994; O'Connor et al., 1994; Clague and Evans, 2000; Procter et al., 2010).

3.3.1. Palaeohydraulic reconstruction

The simplest form of hydraulic modelling involves the use of palaeocompetence and palaeohydraulic techniques to reconstruct flood stage and discharges, typically at the reach scale (e.g. Costa, 1983; Williams, 1984; Kershaw et al., 2005; Bohorquez and Darby, 2008). Using this method, empirical equations are used to relate clast size to hydraulic parameters. When combined with measures of cross-sectional channel geometry, longitudinal channel slope, and roughness coefficients of the reach in question (known as the 'slope-area' method), these relationships are capable of providing estimates of peak discharge and flood velocity for 'steady' hydraulic conditions, where it is assumed that hydraulic variables including flow depth, velocity, and discharge may vary at successive points downstream, but are considered as remaining temporally constant (Riggs, 1976; Williams, 1978; Costa, 1983; Baker, 1988; Baker, 2000). In reality, GLOFs are inherently 'unsteady' and are typically characterised as exhibiting spatially and temporally varying flow discharges, velocities, stage and sediment transport conditions.

3.3.2. GIS-based methods

The simplest computational models are GIS-based flow-routing algorithms, which transfer flow sequentially downslope across a digital elevation model (DEM) (e.g. Desmet and Govers, 1996; Liang and Mackay, 2000). Modified single-flow (MSF) models assign flow from a cell to one of its eight neighbours (the 'D8' method), based on the direction of steepest descent (O'Callaghan and Mark, 1984). The obvious limitation of this method is its inability to transfer flow to more than one adjacent cell (Tarboton, 1997). Accordingly, more advanced algorithms are capable of allocating the contents of a given cell to its neighbours (the 'multiple-flow direction' (MF) model, weighted according to slope angle. MSF and MF models also assume a critical slope angle, below which runout will cease (Huggel et al., 2003). Such models have seen an appreciable amount of use in the natural hazards literature, most likely as a result of their general applicability to many types of gravitational flows (e.g. Huggel et al., 2008). Their use in GLOF simulation has been rather more limited. Relevant studies include the work of Huggel et al. (2002b, 2003), who used a combination of MSF and MF modelling to simulate outbursts from a number of lakes in the Swiss Alps and the Peruvian Andes, and Allen et al. (2009), who used MSF modelling to investigate potential ice avalanche-debris flow interactions and flood hazard in Mount Cook National Park, New Zealand.

3.3.3. One-dimensional numerical modelling

Numerical models used for flood reconstructions may be broadly subdivided according to their dimensionality. One-, two- and three-dimensional models (hereafter referred to as 1-, 2-, and 3-D, respectively) are more process- and physically-based than their GIS counterparts, and attempt to solve modified versions of the Navier–Stokes equations (see Batchelor, 1967). 1-D flood routing models are based on a one-dimensional version of the St-Venant, or 'shallow water' equations (SWE) (Barré de St-Venant, 1871):

$$\frac{\partial Q}{\partial x} + \frac{\partial A}{\partial t} = 0 \tag{4}$$

$$\frac{1}{A}\frac{\partial Q}{\partial t}+\frac{1}{A}\frac{\partial}{\partial x}\left(\frac{Q^2}{A}\right)+g\frac{\partial h}{\partial x}-g\left(S_0-S_f\right)=0 \quad (5)$$

where Eq. (4) and Eq. (5) are the conservation of mass and conservation of momentum equations respectively. Q is flow discharge, A the cross-section surface area, t is time, g is gravitational acceleration (9.81 m/s), h is the cross-sectional averaged water depth, S_0 is the longitudinal bed slope, and S_f is the friction slope.

One-dimensional models typically use the step-backwater procedure. This is essentially an automated, numerical adaptation of the slope-area method, with model output comprising energy-balanced water surface profiles (a function of discharge, channel roughness and channel geometry), cross-sectional averaged velocity and discharge (e.g. USACE, 2010). Cross-sectional profiles may be either derived from field surveys, or using a DEM with sufficiently high spatial resolution. Flow may be modelled as either subcritical (wave velocity > flow velocity), supercritical (wave velocity < flow velocity), or as a mixed regime. As well as predefined cross-sections, initial boundary conditions include either an input hydrograph at the uppermost cross-section, or, if unavailable, downstream water profiles calculated either from direct measurement during a flood event, or using palaeo-stage indicators (PSI). The latter approach has typically been used for GLOF reconstruction (e.g. Cenderelli and Wohl, 2003; Kershaw et al., 2005; Bohorquez and Darby, 2008), as high discharges and flow velocities, turbulence, and the inclusion of large clasts renders them virtually impossible to instrument, particularly in upper reaches. Consequently, the few directly measured GLOF hydrographs that exist are from locations tens or hundreds of kilometres downstream where relatively subdued flow dynamics permits instrumentation (Richardson and Reynolds, 2000a). Popular freely or commercially available 1-D models that have been used in the glacial hazards literature include HEC-RAS (Cenderelli and Wohl, 2001, 2003; Alho et al., 2005; Alho and Aaltonen, 2008; Carling et al., 2010; USACE, 2010), and the NWS DAMBRK (Meon and Schwarz, 1993) and FLDWAV models (Bajracharya et al., 2007).

3.3.4. Higher-order numerical modelling

Two-dimensional models are based on depth-averaged versions of the SWE, derived by integrating the Reynolds-averaged Navier–Stokes equations over the depth of the flow (Chanson, 2004; Hervouet, 2007). Advantages of using 2-D models include their ability to simulate multi-directional and multi-channel flows (in contrast, and as their name implies, 1-D models are only capable of routing flow in one direction, i.e. downstream), super-elevation of flow around channel bends, hydraulic jumps (i.e. in-channel transitions between supercritical and subcritical flow regimes) and turbulent eddying. These are dynamic characteristics intrinsic to GLOFs. Two-dimensional models are often capable of simulating non-Newtonian flow dynamics (e.g. Pitman et al., 2013) such as those observed when a GLOF has entrained a volume of debris from the moraine-dam and valley floor to sufficiently alter its flow rheology (see e.g. O'Brien, 2003; Rickenmann et al., 2006; Armanini et al., 2008; Stoltz and Huggel, 2008). Fully 3-D models are capable of solving the full Navier–Stokes equations, resulting in calculation of variations in flow velocity across both the flow width and depth. Despite their representation of the more complex hydraulic and sediment transport characteristics of catastrophic flooding, to date 2-D and 3-D modelling applications in the flow hazards literature are rare (e.g. Worni et al., 2012), with the majority of studies focusing on glacial outburst floods (jökulhlaups) (e.g. Carrivick, 2006, 2007; Alho and Aaltonen, 2008; Bohorquez and Darby, 2008), or mudflows (e.g. Stoltz and Huggel, 2008; Boniello et al., 2010). This paucity of 2-D and 3-D model applications to GLOF simulation most likely stems from the coupling of high computational cost and the lack of DEMs at sufficiently fine resolution in alpine areas to make their use tractable.

4. Contemporary modelling challenges

4.1. Dam-breaching

4.1.1. Modelling breach initiation

From a modelling perspective, a high degree of uncertainty surrounds the breach formation stage. This is largely attributable to the lack of incorporation of detailed simulations of erosion and breach flow in existing breach models (Wahl, 1998, 2004). During breach formation, rates and patterns of erosion and outflow vary considerably. Recent reviews (Wahl, 1998; Mohamed et al., 2002; Morris et al., 2008, 2009b) highlight the importance of the 'breach initiation' phase, defined as a period of relatively minimal, but increasing discharge, during which dam integrity is yet to be compromised (Fig. 6). Through intervention, runaway breach expansion may be avoided at this stage. Though currently lacking, this information is central to the construction of hazard assessments that aim to quantify flood wave arrival times, discharge, and patterns of inundation, all of which are often subject to a significant degree of uncertainty due to the necessary assumptions made during model parameterisation. For overtopping-type failures, breach initiation is typically manifested as the progressive development of an outflow channel by sheet flow over the dam (for non-cohesive material) or a number of channels on the downstream face of the moraine dam (for cohesive material) (Balmforth et al., 2008; Morris et al., 2008). For cohesive material, subsequent overtopping promotes the progressive enlargement of one or more of these channels through headcutting. The breach initiation phase ceases once runaway incision of an outflow channel begins. The length of this period is controlled by a number of factors, including the water depth and return period of overtopping waves, as well as the erodibility of dam material (e.g. Broich, 2002; Balmforth et al., 2008, 2009). Empirical regression equations capable of providing estimates of time to peak (e.g. MacDonald and Langridge-Monopolis, 1984) have been derived almost exclusive from case study datasets of man-made embankment dams, and provide no estimate of breach initiation time.

The delineation of the breach initiation and breach formation phases for failures initiated by seepage and piping within a natural dam is extremely challenging (Wahl, 2004). With the exception of the work of, for example, Fell et al. (2003) and Wan and Fell (2004), our understanding of breach initiation via internal piping and seepage is rather limited, though it has been established that breach initiation via subsurface pathways are typically lengthy (potentially >24 h) and less evident to the casual observer than for overtopping-type failures. The transition from 'normal', clear-water seepage outflow to cloudy seepage with minimal variation in discharge indicates a developing pipe, and thus the beginning of breach initiation (Wahl, 2004). Catastrophic failure cannot be avoided once the overlying material collapses under its own weight and subsequent erosion in the style of an overtopping failure occurs (Mohamed et al., 2002).

For moraine dams, the presence of interstitial ice, ice lenses, a massive ice core, or permafrost (e.g. Hambrey et al., 2009; Worni et al., 2012), introduce further challenges for modellers. Ice cores represent largely impermeable barriers along (or indeed, in the presence of structural discontinuities in the form of relict crevasses traces, through) which subsurface flows are concentrated and routed, accelerating thermal erosion of the ice and removal of overlying sediment (Watanabe et al., 1995; Richardson and Reynolds, 2000b; Janský et al., 2009). Following assessment of the extent of stagnant ice within moraine dams, achievable almost exclusively through the use of in situ geophysical techniques (e.g. Pant and Reynolds, 2000; Richardson and Reynolds, 2000a,b; Reynolds, 2006, 2011), dams may be treated as composite structures, much like artificial rock fill or clay-cored constructions, for the simulation of overtopping failures. However, there is little published evidence of theoretical, physical or computational experimental parameterisation of dam breach models and the exploration of the implications for failure dynamics.

Presently, the breach initiation phase is poorly represented or entirely neglected in breach models (Morris et al., 2008). As an example, the 'time to failure' boundary condition in DAMBRK (Fread, 1984) is defined as the time taken for final breach dimensions to develop once downstream face erosion and subsequent breaching of the upstream dam face has already been achieved. Thus, any detailed simulation or quantification of initiation time is neglected. However, the standalone NWS-BREACH model (nested within DAMBRK), is capable of providing information on elapsed time associated with the transition from erosion of the downstream to upstream face, which may, with caution, be taken as indicative of a switch from the breach 'initiation' to 'development' phase.

4.1.2. Breach enlargement

Significant progress has been made in the last decade through the identification of issues with dam-break model physicality by international working groups, including the CADAM, IMPACT and FLOODsite projects (e.g. Mohamed et al., 2002; Morris et al., 2008, 2009b), as well as the ongoing work of the Dam Safety Interest Group (CEATI, 2012). Although these projects focused predominantly on modelling the failure of artificially-constructed earthen embankment dams, the models considered have seen widespread use in the glacial hazards literature, and so, with careful interpretation, many findings may be equally applicable to moraine dam failure scenarios. Concerning dam-breach formation, a range of issues pertaining to, for example, the mechanics of breach enlargement, side slope evolution and breach flow hydraulics have been identified. Mohamed et al. (2002) highlighted the inability of existing models to accurately simulate the processes of breach widening and enlargement. A constant shape, typically rectangular (e.g. Wetmore and Fread, 1984), trapezoidal (e.g. Cristofano, 1965; Fread, 1984; 1988b) or parabolic (e.g. Harris and Wagner, 1967), and a linear or user-specified rates of development of increase in breach width and depth, are assumed by the majority of existing models (Wahl, 1997). However, logic dictates that subaqueous and subaerial rates of erosion are far from identical, whilst field evidence and physical scale modelling demonstrates that breach side slopes approach near-vertical angles immediately following down-cutting (e.g. Mohamed et al., 2002; Morris et al., 2008). A transition towards a more parabolic or trapezoidal geometry occurs later in the breach formation stage as mass wasting and discrete block failure of the side slopes occurs. The heterogeneous composition and relatively non-cohesive nature of moraine dam material would suggest that maintenance of steep side slopes during breach development is less likely. However, recent large-scale physical dam-break experiments have demonstrated that steep-sided breaches develop for a range of dam compositions, including both non-cohesive and cohesive materials (e.g. Vaskinn et al., 2004).

Following recognition of the limitation of existing models, a number of advanced, commercially- or publicly-available, physically-based numerical breach models have been developed. Notable examples include HR-BREACH (Mohamed et al., 2002; Morris et al., 2008), SIMBA (Temple et al., 2005; Hanson and Hunt, 2007), and BASEMENT (Faeh et al., 2011). As an example of the improved physicality and dimensionality afforded by the use of such models, in combination with standard treatments of hydraulics, sediment transport and soil mechanics, HR-BREACH is capable of iteratively adjusting breach shape through the incorporation of an improved methodology for modelling lateral breach expansion through the simulation of both continuous erosion and discrete mass failure (Mohamed et al., 2002). With the exception of the work of Worni et al. (2012), advanced dam breach models have not been applied to the moraine dam failure problem, but have the potential to vastly improve our understanding of failure dynamics through improved physical representation of complex failure processes and outflow hydrodynamics.

4.1.3. Permafrost and massive ice

Another key parameter, also often overlooked, is the erodibility of dam material (Hanson and Cook, 2004; Hanson and Hunt, 2007; Morris et al., 2008). Sediment transport equations used within the majority of breach models consider the removal of dam material as a function of applied shear stress, water velocity, and particle diameter, which are unrepresentative of the true variables that dictate erodibility (Morris et al., 2008). Dam material texture (including soil cohesivity), compaction moisture content and compaction energy exert a profound influence over erodibility, and, along with dam geometry, determine headcut migration rates during breach initiation. Indeed, small changes in moisture content or compaction have been shown to result in order-of-magnitude changes in erodibility (Hanson and Hunt, 2007; Morris et al., 2008). Ideally, in situ investigation of the above variables is desirable, however, due to logistical challenges these are often estimated. Quantification of erodibility coefficients for materials typically used for the construction of embankment dams (soil/clay mixtures) has been attempted (Hanson and Hunt, 2007), though such material differs significantly from glacial moraine, which is typically non-cohesive, poorly consolidated, composed of a heterogeneous mixture of sand, gravel, cobbles, and boulders (e.g. Benn and Owen, 2002) (Fig. 4), and may contain discontinuous or continuous permafrost and cores of massive, relict ice (e.g. Hanisch et al., 1998; Reynolds, 2000; Richardson and Reynolds, 2000a; Delisle et al., 2003; Hambrey et al., 2009).

The potential presence of a range of permafrost concentrations and structures represents a significant modelling challenge. There is no evidence in the literature of experimental or field-based investigation into the erodibility of glacial moraine dam material, including the influence of ice content on breach development, having been undertaken to date. Recent research into the degradation of frozen river-bank sediment reveals complex degradational patterns between thawed, frozen and massive ice-cored material (Dupeyrat et al., 2011). Dupeyrat et al. (2011) discovered that the resistance of pure ice to thermal erosion by flowing water was greater than that of surrounding permafrost with lower ice content. Following the ablation of interstitial ice, cohesion and therefore substrate shear strength is vastly reduced, facilitating the rapid removal of sediment (Gatto, 1995). Equally, the importance of discrete mechanical instead of thermal erosion mechanisms increases with the bulk density of permafrost (Lick and McNeil, 2001; Dupeyrat et al., 2011). A critical ice content may therefore be identified, above which mechanical failure dominates, and below which progressive ablation and sediment removal is the main mode of erosion. At present, even the most advanced dam breach models are unable to account for the presence of permafrost or massive, 'pure' ice in the dam structure, though this may indeed prove to be a controlling factor on rates of breach development and should be a priority for future experimental and numerical modelling research.

4.2. Hydrodynamic modelling

4.2.1. Multiple flood waves and model coupling

Most retrodictive or predictive GLOF modelling efforts have considered breach enlargement and the downstream routing of the escaping floodwaters as a single event. However, a number of historical GLOFs have been identified as multiple-phase events (e.g. Clague et al., 1985; Vuichard and Zimmerman, 1986; Clague and Evans, 2000; Kershaw et al., 2005). Depending on displaced water volume and the degree of flow attenuation as the moraine crest is traversed, single or multiple overtopping wave may represent self-contained flood events, regardless of whether this eventually leads to breach formation (e.g. Hubbard et al., 2005; Kershaw et al., 2005). To simulate this phenomenon, the modeller is first required to estimate the overtopping flood hydrograph for entry as an upstream boundary condition. Since contemporary dam breach or flood routing models are generally incapable of performing such calculations, overtopping volume and duration must be calculated independently using known (or estimated) input mass, basin and dam parameters applied to the empirically-derived equations of, for example, Muller (1995) or Walder et al. (2003). Results may then be used to force model applications to determine the flood

characteristics of the initial escaping floodwaters. Similarly, the temporary armouring or blockage of the moraine breach by discrete mass failure of the breach sidewalls or blocks of ice (e.g. Worni et al., 2012) may contribute to the intermittency and 'pulsing' of the escaping floodwaters, such as that documented by Vuichard and Zimmerman (1986) for the 1985 Dig Tsho GLOF. Whilst physically based numerical dam-breach models are capable of simulating discrete mass failure and the subsequent removal of this material by the breach flow, numerical reconstruction of the intermittency of breach expansion and hydrograph development remains challenging in a modelling environment which is typically unable to numerically resolve individual clasts and boulders.

A further complication for the preservation of flow hydraulics and sediment transport is the nature of model coupling. The NWS DAMBRK and FLDWAV codes comprise both dam breach and flow routing algorithms (Fread, 1993). Similarly, HEC-RAS permits the breaching of an inline structure, either at the source of the flood (e.g. at the exit of a reservoir or storage area), or at a user-defined point along the flow path (USACE, 2010). However, both approaches use parametric-type breaching models, which, for reasons discussed above, represent rather simplified approximations of the breaching process. More traditionally, standalone breach models have been used to produce the initial outflow hydrograph, which is then considered as an upstream input to subsequent hydrodynamic modelling efforts. At present, such an approach is standard practice, though it has implications for the conservation of flow momentum at the dam foundation–valley floor boundary. Here, flow accelerates under the combination of the effects of gravity and the pressure of the overlying water contained in the reservoir (the 'pressure head') (Carrivick, 2010). In a fully-coupled, higher order model, short-lived flow acceleration, and a resulting zone of intensely turbulent flow at the dam base would be preserved. However, such effects are not considered when breaching and flood routing models are decoupled. Consequently, near-dam flow velocities calculated using this method are likely to be underestimated.

A related and equally important consideration is the conservation of sediment outflow dynamics at the exit of the breach, and use as input to hydrodynamic modelling. Many studies have largely failed to acknowledge or account for this, yet from a geomorphological perspective, and in combination with outflow discharge and flow hydraulics, the erosion and subsequent transport of morainic material from the breach controls the transience of patterns of erosion, deposition, and flow rheology (e.g. Kershaw et al., 2005; Worni et al., 2012), particularly in near-field locales. An example of a simulated sediment outflow time series for a Himalayan GLOF, produced using HR-BREACH, is displayed in Fig. 7. In this particular instance, sediment evacuation rates were approximated by calculating the volumetric change of the breach between successive 10 second time steps over the full duration of the simulation. The significant variability in sediment outflow over extremely short time scales (often between individual time steps) is the result of instantaneous, discrete mass failure events which represent the main lateral expansion mechanism of the breach. Such behaviour would most likely be manifest in a hydrodynamic simulation of downstream flood propagation as a series of short-lived sediment 'pulses'. The rheological, hydraulic, and geomorphological effects of temporally-varying flow sediment concentrations are discussed in further detail in Section 4.2.3.

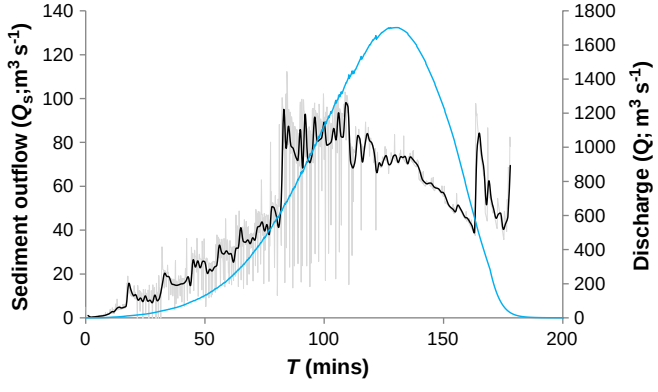

Fig. 7. Rates of sediment evacuation (Q_s) during moraine breaching; in this instance an experimental reconstruction of the 1985 Dig Tsho event using HR-BREACH. Sediment outflow fluctuates significantly between successive 10 second time-steps, as a result of periodic discrete breach wall failure events, which represent considerable, though short lived 'pulses' of sediment to the developing outflow channel. It is worth noting that peak sediment outflow precedes peak discharge (Note: end of sediment time series data corresponds with cessation of breach outflow).

4.2.2. Complex flow hydraulics

As with other sudden onset, sediment-laden outburst floods (e.g. Carrivick et al., 2010), GLOFs possess highly transient and spatially-varying flow regimes. From a modelling perspective, this introduces a range of challenges, including, but not limited to; an often rapid increase in discharge, high flow velocities and rapidly expansive patterns of inundation; the propagation of a translatory shock wave over initially 'dry' terrain; highly turbulent, typically overbank flow, the occurrence of flow super-elevation at sharp channel bends (often triggering secondary failure of colluvial slopes), and highly transitory flow rheology, which exerts a major control over intra- and post-flood channel reworking.

During breach development, escaping floodwaters accelerate under the combination of the effects of gravity and the pressure of the overlying water contained in the reservoir (Stansby et al., 1998). This acceleration is typically short-lived, as floodwaters descending the distal face of the moraine dam encounter comparatively shallow gradients in the proglacial environment. Given a wide, largely unconfined proximal zone, flow will expand laterally as sheet flow, with depth and velocity gradually decreasing with distance from the flood source (Cenderelli and Wohl, 2003; Hogg and Pritchard, 2004). Alternatively, the continuation of steep near-field topography will promote the convergence of floodwaters, producing a higher velocity initial flood wave. As the flood wave propagates downstream, time-varying flow discharges and depths, combining to determine the overall degree of inundation, will be dictated by the breach outflow hydrograph and topographic complexity.

One-dimensional hydrodynamic models are unable to simulate many key characteristics of GLOFs. Energy losses through the effects of boundary friction and turbulent eddying is handled explicitly in 2-D and 3-D flow models, though are accounted for in 1-D models through representations of channel conveyance. This is typically undertaken through manual calibration of roughness coefficients, such as Manning's *n*, in order to produce optimal, or 'best-fit' water surface profiles to palaeo-stage evidence, or at-a-point hydrographs which closely mirror available observed data (usually unobtainable) (e.g. Cenderelli and Wohl, 2001; Bohorquez and Darby, 2008). No studies currently exist which directly compare the application of 1-D and 2-D hydraulic models to the GLOF phenomenon. However, analogous research has been undertaken for glacial outburst floods, including the work of Alho and Aaltonen (2008) and Bohorquez and Darby (2008). The former found that, for unsteady outburst flow simulations across a relatively wide, shallow Icelandic *sandur*, predicted inundation extents were broadly comparable, with the greatest discrepancies occurring when flow encountered a sinusoidal gorge (Alho and Aaltonen, 2008). On the face of it, and with careful calibration, these findings appear to encourage the use of expeditious, computationally undemanding 1-D models, though *sandar* are often far less topographically complex than steep, high relief and tortuous alpine channels. However, Bohorquez and Darby (2008) found that a 1-D model compared reasonably to a 2-D approach for a glacial outburst flood in a high mountain, alpine setting. Averaged discharge estimates produced using 1-D modelling were higher than equivalent data obtained through 2-D modelling (429–557 $m^3 s^{-1}$ and 358–454 $m^3 s^{-1}$ for 1-D and 2-D models, respectively),

attributable to the reconstruction of a recirculation zone in the 2-D model, which the 1-D model was unable to reproduce due to its inherent unidirectional treatment of flow direction (Bohorquez and Darby, 2008). This particular example was undertaken over a relatively short distance (<1 km), and for an outburst event with a peak discharge an order of magnitude lower than many documented GLOFs. The natural question arising from the above therefore becomes: how do spatio-temporal fluctuations in GLOF dynamics, including the timing and maximum extent of flood inundation, vary with model dimensionality? With the increasing use of advanced hydraulic codes, a comprehensive appraisal of 1-D, 2-D and 3-D approaches to GLOF prediction is a fundamental research priority, and will be of key interest to hazard assessment and disaster mitigation bodies who are considering the use of more advanced codes.

As far as possible, and regardless of model dimensionality, particular attention should be given to the numerical discretisation of the flow path in a sufficient level of detail (Fig. 8). A sufficiently detailed topographic representation of the flow path is central to the production of meaningful, robust estimates of flood duration, discharge, velocity, and inundation extent, and is a prerequisite for the use of 2-D and 3-D hydrodynamic models. This is of particular importance in upper reaches, where, for a range of hydrograph forms, flood dynamics may vary significantly. However, results of the intercomparison of coarse (e.g. SRTM) versus fine (e.g. LiDAR) topographic data for flood inundation modelling (e.g. Sanders, 2007) have revealed that coarse-resolution elevation data possess remarkable value, particularly for rapid, 'first-pass' assessments. Similarly, Huggel et al. (2008) discovered that coarse SRTM and ASTER terrain data, in combination with GIS-based flood routing models, possess remarkable value for providing first-order hazard assessments of volcanically triggered lahars.

The increasing availability of affordable, high-specification desktop computing resources means that the reconstruction and adoption of detailed floodplain topography (and higher order hydrodynamic models) is becoming increasingly viable (e.g. Alho and Aaltonen, 2008; Carrivick et al., 2010). However, the acquisition of fine-resolution topographic datasets is often significantly hindered in many remote, inaccessible, high-altitude regions due to logistical impracticalities. Recent advances in the development and provision of free, publicly-available and user-friendly photogrammetric methods (e.g. Westoby et al., 2012), and the increasing affordability of low-altitude tethered (e.g. Boike and Yoshikawa, 2003; Smith et al., 2009; Vericat et al., 2009) and autonomous surveying platforms (e.g. Lejot et al., 2007; Niethammer et al., 2012) are steadily making the production of high-resolution topographic data products for (geo)morphological analysis and grid-based representation of alpine valley floor topography more practical.

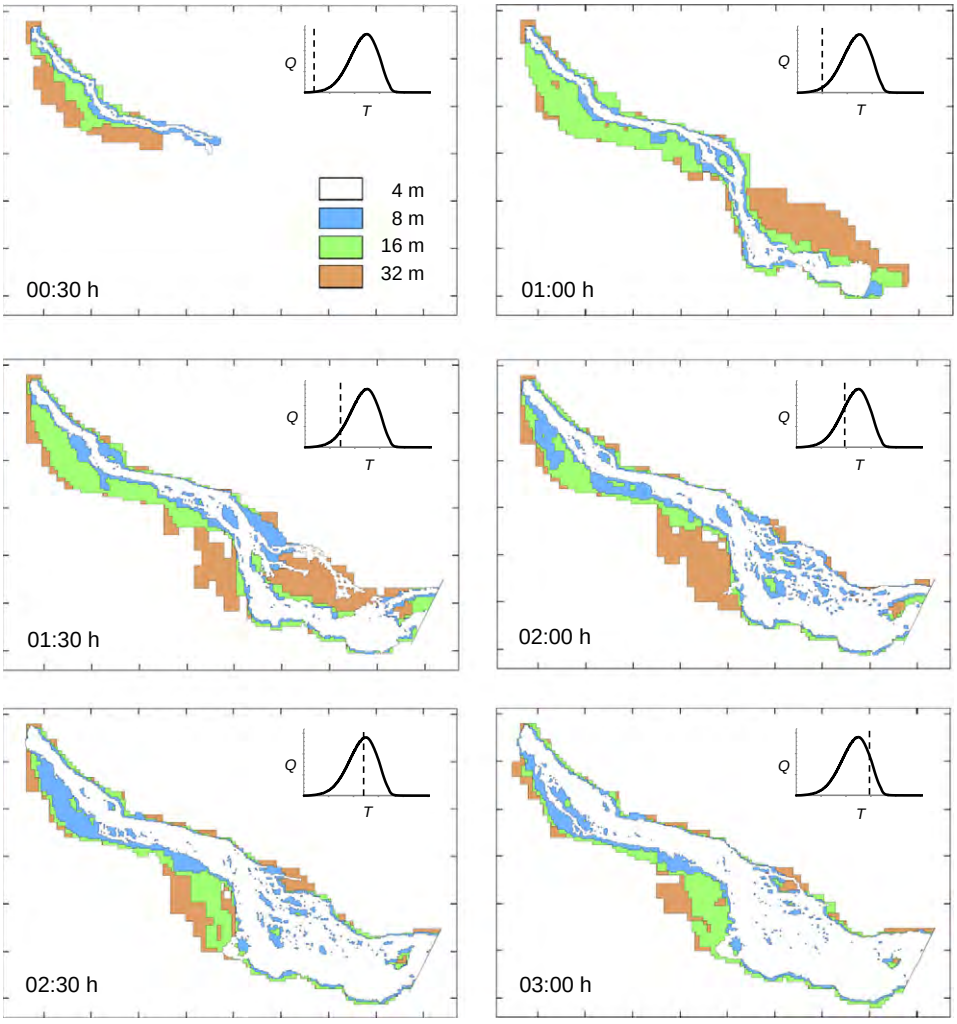

Fig. 8. Flood inundation extent at selected time steps for the two-dimensional hydrodynamic reconstruction of a palaeoGLOF from Dig Tsho, Nepal Himalaya using a Total Variation Diminishing solver (ISIS 2D). Topographic grid discretisations of 4 m, 8 m, 16 m and 32 m were used. The 4 m and 8 m results are broadly comparable for all time steps, whereas use of 16 m and 32 m grids results in the inundation of sizeable areas of the valley floor otherwise unaffected by GLOF passage across the finer grids. Dashed line on inset box shows corresponding time step on the breach outflow hydrograph (for reference, this is identical to the 'optimal' hydrograph shown in Fig. 7). For scale, tick marks on main figure spaced at 200 m intervals.

4.2.3. Multi-phase flow and the mobile bed problem

In combination with downstream topographic complexity, flow bulking through the erosion and entrainment of valley floor and morainic sediment often results in the breach outflow hydrograph being largely unrepresentative of downstream flood discharges (e.g. Cenderelli and Wohl, 2003; Kershaw et al., 2005). This is especially the case for flows which rapidly transform into sediment-laden hyperconcentrated or debris flows. In investigating the failure of Neoglacial moraine dams in the Cascade Range, Oregon, O'Connor et al. (2001) estimated that GLOFs transformed from clear water to debris flows within 0.5 km of their source, with the total volume of water released believed to have comprised >25 percent sediment. This is unsurprising, given the vast quantities of unconsolidated glacial and glacio-fluvial material which comprises proximal, deglaciated terrain.

The entrainment of significant volumes of in-channel and overbank sediment has implications for flow mobility. Fundamentally, an increase in flow volume as a result of the addition of solid material will in turn increase flow velocity. However, consequent increases in flow viscosity and cohesion may act to reduce mobility (Breien et al., 2008). Experimental work by Iverson et al. (2011) revealed that flow mobility decreases with the passage and entrainment of sediment over initially dry terrain. However, if the flow overrides and entrainments sediment from initially wet terrain, flow bulking, a subsequent increase in flow speed and momentum, and the development of large positive pore pressures will result (Iverson et al., 2011). Research in the Swiss Alps by Haeberli (1983) and Huggel et al. (2002a) revealed that minimum average slopes of 11° and 2–3° are required for the sustained runout of debris flows and clear water flows, respectively, reinforcing the largely demobilising effect of substantial sediment entrainment and transport. Consequently, the presence of complex channel topography will result in periodic, transitory fluid dynamics.

From a modelling perspective, simulation of the above is highly challenging. As well as neglecting the contribution of transversal velocity to the flow momentum balance, relatively simplistic MF or MSF flow routing algorithms and the majority of 1-D hydrodynamic models are incapable of simulating non-Newtonian flow rheology. This is a fundamental characteristic of sudden onset floods, and has been documented for GLOFs (e.g. Clague and Evans, 2000; O'Connor et al., 2001; Breien et al., 2008), landslide-dammed lake outburst floods (e.g. Capra and Macías, 2002; Dunning et al., 2006; Xu et al., 2012), jökulhlaups (e.g. Carrivick, 2006, 2007), mudflows (including volcanically-triggered lahars) incorporating high concentrations of volcaniclastic material (e.g. Manville, 2004; Carrivick et al., 2009, 2010), and hyperconcentrated or debris flows caused by a rock or ice avalanche (e.g. Hubbard et al., 2007).

Entrained sediment affects flow density, viscosity and turbulence. Short-lived changes in hydraulic regime, including the direct influence of sediment on flow hydraulics (e.g. Carrivick, 2010) and concurrent channel reworking, represent major challenges for numerical modelling. Consequently, these effects commonly remain largely overlooked and unquantified (Carrivick et al., 2011). Research into flow-sediment interactions in sudden onset floods with a dam failure origin has been necessarily confined to laboratory-scale investigation (e.g. Chen and Simons, 1979; Capart and Young, 1998; Nsom, 2002; Rushmer, 2007; Carrivick, 2010; Laurent et al., 2011), where issues of scaling and the confined nature of the flow should be considered (Carrivick et al., 2011). A key finding has been the discovery that, in the early stages of the flow event, and without sufficient time to reach capacity, floods where suspension is the predominant mode of sediment transport exhibit a 'dynamic equilibrium' regime. This is manifested geomorphologically as alternating zones of erosion and deposition (Carrivick et al., 2010; Procter et al., 2010), whereby initially high rates of erosion and sediment entrainment and transport rapidly give way to a depositional regime as the transport capacity declines as a function of energy losses through boundary friction and geomorphic work (Carrivick et al., 2011). The results of numerical modelling presented by Xia et al. (2010) suggest that, at least in the initial stages of outburst flood propagation, rates of bed evolution and scour may approach or equal flow depth.

Processes of fluid flow and sediment transport are inherently linked to bed evolution. The vast majority of models currently in widespread use are only capable of routing floods over an immobile bed (Liao et al., 2007; Xia et al., 2010). The 'mobile' bed problem describes the propensity for the channel bed to undergo continuous morphological change over the course of an event, including the large-scale mobility of the underlying substrate through tractive or rolling motion. Consequently, the physical manifestation of the channel 'bed', as classically defined, becomes blurred, as a continuum develops comprising fluid, often intensely sediment-laden flow, a zone of active bed mobility and bed-flow sediment exchange, and underlying immobile substrate. A number of models capable of solving the mobile bed problem for dam break floods are reviewed in Xia et al. (2010), and are not described in detail here, however, advances in our understanding of the processes that govern this behaviour have been largely experimental (e.g. Cao et al., 2004; Simpson and Castelltort, 2006; Leal et al., 2009; Xia et al., 2010; Zhang and Duan, 2011). Key findings include the observation that flows over a mobile bed attenuate faster (Carrivick et al., 2011), and peak flow depth was greater and occurs earlier than for those over an immobile bed (Leal et al., 2009).

GLOF modelling efforts that account for the presence of a mobile bed layer in their numerical solutions are rare. Analogous studies include the work of Xia et al. (2010), who document the development and application of a 2-D morphodynamic model capable of considering the influence of flow sediment concentration and bed evolution on flow propagation, as well as the work of Carrivick et al. (2010) who utilised a 2-D fluid dynamics model, Delft-3D, to reconstruct time-varying patterns of geomorphic change produced by a crater lake break-out lahar in New Zealand. Although the model is unable to simulate changes in flow rheology as a result of varying sediment concentration, the capability of Delft-3D to handle prior specification of zones of active (i.e. alluvial) and inactive (i.e. bedrock) channel substrate and actively update cell-specific sediment quantities renders it highly suitable for the investigation of intra- and post-event channel reworking (Carrivick et al., 2010), though has yet to be applied to the simulation of GLOFs. The above findings may have significant implications for the use of purely hydrodynamic models for GLOF reconstruction and prediction, which fail to incorporate solutions of sediment erosion and transport, including spatio-temporal variations in flow rheology and hydraulics and mobile bed evolution.

4.2.4. Mesh-free methods for dam-breach simulation

The various methods presently thus far belong to the 'mesh-based' category of hydrodynamic models for open channel flow. Over the past decade or so, a range of particle-based, mesh-free methods for modelling complex fluid flows have been developed. Of these, the 'smoothed-particle hydrodynamics' (SPH) approach is perhaps the most popular (e.g. Bursik et al., 2003; Cleary and Prakash, 2004; Laigle et al., 2007; Pastor et al., 2009; Liu and Liu, 2010; Huang et al., 2012; Kao and Chang, 2012). SPH is a truly mesh-free, Lagrangian, particle-based method for solving the classic mechanics of fluid flow; typically the Navier–Stokes equations. Flows are discretised into a finite number of elements, or particles, possessing predefined geometric and material properties, and inter-particle contact laws (Cleary and Prakash, 2004). Particles are not truly physical, but, when grouped, are considered as a means of representing the fluid(s) under investigation (Laigle et al., 2007).

Fully 3-D fluid dynamics, including treatments of local flow density and vertical acceleration, are simulated through inter-particle interactions, which are determined by spatial weighting or smoothing functions (Liu and Liu, 2010). When interacting *en masse*, SPH methods have been demonstrated to reproduce complex, often transient phenomena of natural fluidal flows, including supercritical, subcritical, and

transcritical flow regimes, hydraulic jumps, shock wave propagation, wave reflection and multiple wave interactions, and splashing and flow fragmentation (Chang et al., 2011; Kao and Chang, 2012), even at relatively coarse resolutions (Cleary and Prakash, 2004). In addition, dynamic free-surface behaviour (e.g. flow superelevation) is handled with ease and without the requirement for the use of surface tracking methods (commonly required by purely mesh-based models). SPH is capable of simulating rheologically complex, non-Newtonian flows with ease, including flow solidification and fluidisation behaviour, making it ideal for application to natural flows which have been shown to demonstrate transient flow rheologies.

The above capabilities render SPH highly suited for the investigation of sudden onset, dam-break floods. To date, the use of mesh-free methods has been largely confined mainly to experimental application against standard benchmarking problems (e.g. Chang et al., 2011), although a number of real-world case studies have been investigated. These have included the routing of dam break outburst floods over DEMs of varying topographic complexity (e.g. Chang et al., 2011) and modelling hypothetical landslide runout (Huang et al., 2011, 2012), including dynamic landslide-reservoir interactions (Pastor et al., 2009). The work of Pastor et al. (2009) is broadly analogous to the direct interaction of rock or ice avalanches with moraine-dammed lake complexes, and represents a holistic, multi-component approach to modelling all of the phenomena involved, including mass movement trajectory modelling, the interaction of a landslide or avalanche with the lake body and near- and far-field wave propagation. The addition of a treatment describing subsequent wave overtopping of a natural dam structure would complete the unified simulation of all initial stages of this particular trigger mechanism, and is an approach that merits further methodological exploration. The application of mesh-free methods to the simulation of GLOFs is a natural progression from the use of the depth-averaged 1-D and 2-D methods described above. Initial concerns over issues of model validation and computational efficiency (e.g. Richards et al., 2004) appear to have been overcome in some instances, with a number of SPH codes have been shown to perform with favourable computational efficiency and reliability (e.g. Chang et al., 2011). However, examples of SPH application to 'large-scale' simulations such as the routing of dam break outburst floods through lengthy, topographically complex catchments, such as those found in high mountain regions, are currently lacking.

4.3. Implications for Glacial Lake Outburst Flood modelling

The strengths and inadequacies of the models described above must be considered by workers attempting to reconstruct palaeoGLOFs or simulate future, hypothetical outburst events. Ultimately, the choice of modelling approach will be dictated by logistical and financial constraints. From a practical perspective, a relatively simple, purely raster- and DEM-based approach will be more appealing to workers tasked with the production of first-order assessment of the hazard posed by GLOFs at the regional scale (e.g. Huggel et al., 2003; Allen et al., 2009) and particularly in remote regions where high-resolution terrain data are currently unavailable. Such models represent a low-cost and computationally-undemanding method for modelling the downstream propagation of GLOFs, favour the use of simple, empirically-derived estimations of Q_p and T_p (e.g. Table 3), and are suitable for use in combination with coarse-scale terrain data for 'first-pass' hazard assessments (e.g. Huggel et al., 2003).

Increasing model complexity is traditionally associated with increases in initial start-up costs. Although also relatively computationally undemanding, more advanced models typically require a corresponding increase in user expertise and data requirements for effective parameterisation and implementation. Many input parameters, particularly material characteristics of the moraine dam, are only obtainable through labour-intensive and logistically challenging field investigation (e.g. Xin et al., 2008; Worni et al., 2012), although the well-documented heterogeneous nature of moraine dams (Benn and Owen, 2002; Bennett and Glasser, 2009; Hambrey et al., 2009) may hinder a single, definitive quantification of their material properties at all. Theoretically, improved representation of the varied and complex physical characteristics of breaching and flood propagation through the application of, for example, analytical or parametric dam breach models and 1-D depth-averaged hydrodynamic solvers are likely to improve the accuracy and robustness of spatial and temporal predictions of inundation and GLOF dynamics in some instances. However, the lack of a consideration of key dynamical aspects of GLOF behaviour, such as turbulent, often super- or transcritical flows, flow superelevation at channel bends, and transitory flow rheologies still serves to limit the veracity and precision of these approaches.

Higher-order modelling approaches, including the use of next-generation dam breach models and 2-D, 3-D, or mesh-free hydrodynamic models currently represent the most advanced, physically-robust approaches to GLOF modelling. Traditionally, the use of such models has required a significant degree of user expertise, though accessibility has steadily improved in recent years with the increasing use of Graphical User Interfaces (GUI) and GIS support to simplify data input, manipulation and visualization. However, this is offset somewhat by the high initial start-up costs of many codes, the majority of which are distributed as proprietary software packages. In addition, significant computational requirements render them largely unsuitable for the investigation of input parameter uncertainty and equifinality in model output through the use of Monte Carlo methods, for example. For this purpose, simpler models are at a distinct advantage until the affordability and use of high-speed parallel computing systems or high-specification desktop computers becomes more commonplace, or models become more computationally efficient.

4.4. Challenges posed by contemporary and future climatic change

Rates of glacial recession are predicted to increase in the coming decades on a scale without any known historical precedent (IPCC, 2013). Consequently, and in addition to the challenges discussed above, we will be increasingly faced with challenges associated with modelling GLOF events and glacial and geomorphological conditions to which our range of empirical observations may no longer apply.

One of the major challenges is predicting where future glacial lakes will form. On debris-covered glaciers, a specific set of glaciological conditions which predispose a glacier to develop a network of supraglacial ponds, and ultimately a fully formed moraine-dammed glacial lake, have been identified (Reynolds, 2000; Quincey et al., 2007) and form a robust basis for identifying those glaciers which are likely to develop glacial lakes in the future. Similarly, qualitative strategies have been developed for identifying the location of subglacial overdeepenings through analysis of the characteristics of glacier surface topography, which, following glacier retreat, may serve as the focal point for meltwater collection and the development of a proglacial lake (Frey et al., 2010).

However, the rate of observed and predicted future increases in air temperature and variations in the precipitation regime of many high-mountain regions are such that it remains a challenge to predict the pace of future cryospheric change, and how it relates specifically to the development of the GLOF hazard at regional and local scales. Anticipating the celerity with which various glaciological processes will operate, and the timescale required for key physical and climatological thresholds to be exceeded are hindrances to our prediction of the evolution of the GLOF hazard. A prudent approach for assessing the GLOF hazard posed by extant or future moraine-dammed lakes should be based on the regular re-analysis of glaciological, geomorphological and climatological data, with a view to identifying contemporary and future GLOF process chains, and subsequently informing the development or parameterisation of empirical and numerical dam-breach and hydrodynamic models.

5. Considering uncertainty in the GLOF model chain

An appreciable degree of uncertainty surrounds the establishment of initial boundary conditions and input parameters for both reconstructive and predictive dam-breach and GLOF modelling. Few studies have undertaken detailed sensitivity analyses into the significance of this uncertainty on, for example, the form of the breach hydrograph, and subsequent implications for the assessment of the spatio-temporal evolution of the GLOF flood wave(s). In many instances, it may be the case that uncertainty associated with model parameterisation results in greater variability in model output than differences attributable to the use of, for example, 1-D, 2-D or 3-D hydrodynamic solvers. Laboratory-scale experiments (Balmforth et al., 2009) indicate that vastly different final breach widths can be reproduced from near-identical initial breach geometries and compositions, whilst Awal et al. (2010) reported that the magnitude and timing of overtopping waves were dependent on dam geometry (specifically proximal face angle), material composition, and additional factors including ice- and rock-avalanche dimensions. Similarly, in Capart's (2013) analytical dam-breaching solution, peak discharge was discovered to be sensitive to the lake surface area, and highly sensitive to the initial angle of the upstream dam face, effectively highlighting the importance of quantifying such geometric descriptors of the moraine dam as precisely as possible prior to the specification of initial model boundary conditions.

With specific reference to numerical dam-breach modelling, significant uncertainty surrounds the establishment of initial conditions (e.g. dam geometry, reservoir bathymetry and hypsometry), the parameterisation of material characteristics (e.g. grain size distribution data, porosity, density, cohesion, internal angles of friction) and the establishment of suitable computational constraints (e.g. model time step and grid discretisation) (Table 4). Whilst the construction of high-resolution DTMs of moraine dam structures (Westoby et al., 2012), their attendant lake basins (e.g. Robertson et al., 2012; Yao et al., 2012), and downstream valley topography (e.g. Bremer and Sass, 2012) using photogrammetric, laser scanning, or bathymetric surveying techniques has facilitated the extraction of metric data pertaining to, and subsequent accurate characterisation of moraine and lake geometry and down-valley topography, equally robust quantification of the aforementioned material characteristics is typically achievable only through labour-intensive and logistically-demanding fieldwork (e.g. Hanson and Cook, 2004; Osti et al., 2011; Worni et al., 2012). Furthermore, the compositional heterogeneity of moraine dams further complicates the use of a single, 'all-encompassing' material parameter ensemble for applied dam-breach simulation in a range of settings.

Variability in hydrodynamic model output may be attributed to model dimensionality (e.g. Alho and Aaltonen, 2008; Bohorquez and Darby, 2008), spatial resolution and quality (e.g. Sanders, 2007; Huggel et al., 2008), the spacing of successive cross-sections that represent downstream topography (e.g. Castellarin et al., 2009), as well as uncertainty surrounding the parameterisation of channel and floodplain roughness coefficients (Wohl, 1998; Hall et al., 2005, Pappenberger et al., 2005), input boundary condition data (e.g. Pappenberger et al., 2006) and stage-discharge relationships (e.g. Di Baldassarre and Claps, 2011). For event-specific flood reconstruction, systematic calibration of roughness and friction coefficients to produce 'best-fit', or 'optimal' model parameters is standard practice (e.g. Kidson et al., 2006; Cao and Carling, 2002), and may serve to inform their choice for modelling hypothetical future events (e.g. Horritt and Bates, 2002). However, the application of these calibration techniques for reconstructive and predictive GLOF modelling is highly questionable, not least because of the uniqueness of each outburst event and the appreciable unlikelihood of more than one GLOF originating from a given moraine-dammed lake. Standard

Table 4
Sources of uncertainty in the GLOF model chain, the nature of their impact and practiced or proposed measures for their quantification or assessment.

	Source of uncertainty in model input (*) or output (†)	Nature of impact or affected output variables	Solution or measure(s) of addressing
Trigger	* Source and timing	Dimensions and dynamics of overtopping waves (e.g. ice- or rock avalanche trigger); may determine whether runaway breach development is triggered	Desk- or field-based glacial hazard assessment of moraine and surrounding topography; analysis of multi-temporal datasets required to quantify evolution of hazard (e.g. Reynolds Geo-Sciences, 2003; Huggel et al., 2004; Quincey et al., 2005).
Dam-breach modelling	* Moraine dam geometry	Dam height, crest width and distal and proximal dam face slope influence style and rate of breach development	Fine spatial resolution characterisation and quantification of moraine-dam geometry (e.g. Westoby et al., 2012). Ideally undertaken in situ
	* Lake bathymetry and stage-volume relationships	Determines reservoir pressure head and rate of inflow to breach	Bathymetric surveying (extant lakes); photogrammetric or 'data-ready' surveying (e.g. TLS) of drained basins
	* Initial conditions (e.g. dam freeboard, spillway dimensions)	Influences impact of overtopping waves (freeboard); accommodation of escaping floodwaters (spillway dimensions); may ultimately determine whether runaway breach development triggered	In situ observation or analysis of fine resolution aerial or space-borne imagery
	* Material characteristics	Rate of breach development	In situ quantification (preferred); literature-guided parameterisation; probabilistic sampling of parameter space
	* Presence of buried ice in moraine	Rate of breach development; interaction of massive ice core with progression of breach development remains largely unquantified (e.g. Worni et al., 2012)	Geophysical inspection of intact moraine dam; visual (and geophysical) analysis of breached structures.
Hydrodynamic modelling	† Grid discretisation	Decreasing grid resolution results in effective 'smoothing' of small-scale topographic elements; in the first instance determines direction of flow	Undertake detailed sensitivity analysis to quantify impact on inundation extents and wetting-front travel times; attempt to validate results where possible (v. challenging)
	* Channel and valley-floor oughness coefficient(s)	Influences effectiveness of flow conveyance, influence more important at low flows; exerts little control over flow dynamics at high flow stage and velocity	Literature- and field investigation-guided classification; investigate and quantify any functional relationship with topographic grid resolution
	† Complex flow rheology (model physicality)	Will influence flow velocities (and therefore wetting-front travel-time) and erosive potential of the flow	Use of advanced hydrodynamic solvers capable of simulating sediment transport, transient flow rheology and mobile bed evolution
	† Model dimensionality	Simple' codes incapable of simulating lateral transfer of flow momentum and mass. Complex flow dynamics (flow superelevation, development of flow recirculation zones etc)	If detailed GLOF hazard assessment required, use of advanced, 2-D solvers advocated. Raster-based or 1-D solvers suitable for 'first-pass' hazard assessment
	† Model coupling	Model de-coupling results in loss of flow momentum and mass transfer. Importance for determining near-field flow velocities and reworking	Use fully-coupled models to simulate breach development and cascading of floodwaters (and morainic material) from lake basin to the floodplain.

calibration techniques, such as the use of palaeo-stage indicators or slackwater deposits (e.g. Cenderelli and Wohl, 2003; Kershaw et al., 2005; Bohorquez and Darby, 2008) represent one possible approach to flow calibration, but are reach-specific and typically reflect only the maximum flood stage and corresponding inundation extent. Similarly, delineation of channel- and valley-floor regions subject to GLOF passage represents a straightforward method of establishing maximum flood extents. However, a widespread lack of pre-GLOF topographic datasets (for GLOF routing), combined with the inability of many widely-used hydrodynamic codes to simulate complex and highly transient flow rheologies and sediment transport dynamics complicates the use of maximum flood extents to accurately constrain palaeoGLOF dynamics.

A potential solution to the above is the adoption of probabilistic approaches to GLOF reconstruction, which embrace uncertainty in the model chain using stochastic sampling techniques and are capable of quantifying the degree of equifinality in model output. Such methods have appreciated widespread use in the distributed hydrological modelling literature (e.g. Beven and Binley, 1992; Kuczera and Parent, 1998; Lamb et al., 1998; Blazkova and Beven, 2004; Franz and Hogue, 2011), and, with limited modification, would appear to be equally suited to dam-breach reconstruction (Fig. 9) and GLOF inundation mapping (Fig. 10). As an example, quantifying the performance of dam-breach models according to their ability to reproduce the geometry of moraine breaches caused by palaeoGLOFs represents one solution to being able to identify the parameter ranges which may be deemed acceptable, or 'behavioural'. However, significant complications arise with the elucidation of a 'universal' range of input parameters for application to predictive GLOF modelling efforts given the highly site-specific nature of their derivation, and the challenges associated with identifying and reconstructing a large enough sample of GLOFs in a specific region from which to undertake a representative statistical analysis of the key modelling parameters (and their ranges) which exert the dominant influence over breach development and GLOF propagation. Specifically, and in the absence of validation of their suitability to reconstructing observed breach morphologies of other breached moraine dams, a range of tightly-constrained material characteristics that may be capable of reproducing observed breach morphologies at one site may not be readily applicable to accurately predicting the range of breach hydrographs that might arise from the failure of another. Nevertheless, the subsequent production of probability-weighted maps of inundation are arguably of more value for flood hazard and risk assessment, and the use of uncertainty-based techniques for both reconstructive and predictive GLOF modelling merits further consideration.

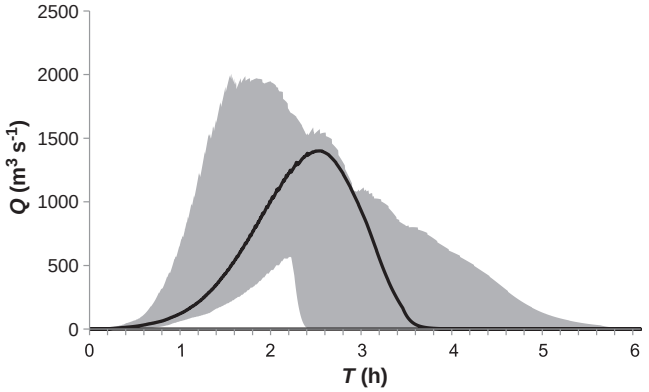

Fig. 9. Dam breach hydrographs for a reconstruction of the Dig Tsho failure. Solid black line corresponds to the 'optimal' breach outflow hydrograph, with performance conditioned on the ability of the simulation to reproduce observed geometric descriptors of post-GLOF breach morphology (including final breach depth and centreline elevation profile or slope). In contrast, grey shading represents the hydrograph envelope of all acceptable, or 'behavioural' failure simulations, reflecting a range of input parameter combinations.

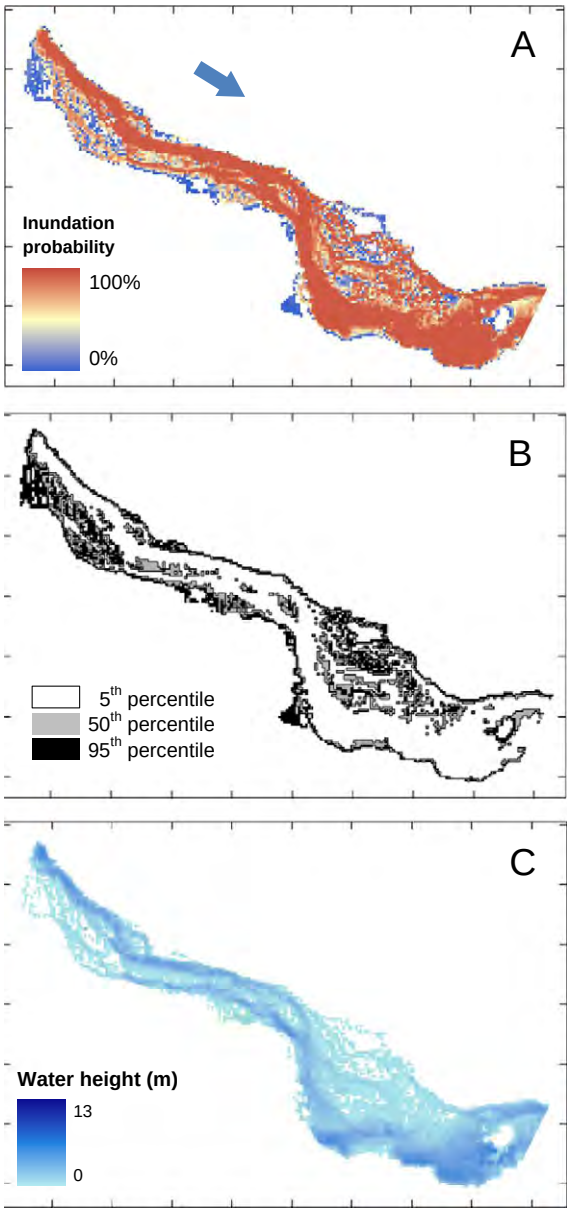

Fig. 10. Communicating uncertainty in reconstructive mapping of the Dig Tsho GLOF. (A) inundation probability, calculated as the percentage of 'behavioural' simulations which inundate a given cell; (B) percentile-specific inundation extent, and; (C) an example of inundation extent and flow depth for the 95th percentile model. All data extracted at 02:00 h after breach initiation. For scale, tick marks spaced at 200 m intervals. Blue arrow in **A** indicates direction of flow.

6. Conclusions

High-magnitude outburst floods from moraine-impounded glacial lakes represent a highly-complex, multi-stage catastrophic phenomenon, capable of accomplishing significant geomorphologic reworking of channel- and valley-floor floodplain environments and posing a very real threat to infrastructure and the safety and livelihoods of communities. This review has provided a comprehensive overview of the individual 'components' that constitute a GLOF event, namely: triggering mechanism(s), moraine dam breaching, and routing of the escaping floodwaters, and the modelling approaches typically used to reconstruct or predict GLOF dynamics.

Progress in understanding of the main factors controlling moraine dam breach dynamics has been relatively slow since the emergence of the first numerical models well over two decades ago. Empirical models,

originally developed for application to the failure of artificially-constructed dams and levees, commonly appear in the geosciences literature and should not be discounted as useful tools for the production of rapid, first-pass hazard assessments. The recent advent of fully physically based advanced numerical dam-breach models heralds a significant step forward in our capability to produce robust, physically based estimates of breach outflow dynamics, including quantification of sediment evacuation rates.

The requirement to model accurately GLOF hydrodynamics at both the source and downstream is central to the production of detailed GLOF inundation maps and hazard assessment. However, the high computational burden associated with the execution of advanced 2-D and 3-D hydrodynamic codes, coupled with the relative dearth of fine-resolution topographic data required for detailed discretisation of channel and floodplain domains are still major hindrances to the widespread adoption of these models for the production of detailed hazard assessments of anticipated GLOF events.

In conclusion, we highlight the following as key modelling challenges and potential areas of future GLOF research.

- The development of dam breach models capable of actively simulating dynamic wave behaviour in a glacial lake, such as those caused by landsliding or avalanching, and accounting for the passage of single of multiple overtopping waves in breach initiation and development;
- Further experimental and numerical investigation into the interactions between seismic activity and the geotechnical performance of moraine dams, specifically its significance in initiating dam settlement or massive structural failure, and the evolution of breach initiation via piping and intra-morainal seepage;
- The ability of dam breach models to use complex, real-world geometric data as input, such as irregular crest topography and arcuate dam planform, providing a true reflection of observed moraine dam geometry;
- Quantification of the effects of spatially continuous or discontinuous permafrost in the dam structure, including massive bodies of relict glacial ice, on patterns of breach erosion, and the development of numerical models capable of accounting for often complex, user-defined spatial variations in ice content.
- Improvements in inter-model coupling, including the preservation of breach outflow hydrodynamics, the passage of multiple overtopping flood waves or breach-flow 'pulses', and temporal variations in sediment evacuation rates from the enlarging breach;
- Quantification of the effects of model dimensionality on reconstructed or predicted flow hydraulics and patterns of inundation and geomorphologic reworking of in-channel and overbank environments, including implications for the construction of downstream hazard assessments;
- Wherever possible, the collection of dam material property and geometric data in situ, in order to constrain dam-breach model input parameters as rigorously as possible, and to reduce the extent of the uncertainty associated with numerical dam-breach model parameterisation;
- The acquisition and use of high-resolution topographic datasets, in order to make the effective use of advanced hydrodynamic models viable, including, where possible, the attainment of pre- and post-GLOF DEMs to aid quantitative analysis and interpretation of net erosion and deposition;
- The adoption of models capable of simulating spatio-temporal patterns of transitory flow rheology, including effects of flow hydraulics and capacity to perform geomorphic work, and the use of models incorporating solutions of mobile bed evolution and subsequent impacts for GLOF propagation.

Acknowledgements

MJW was funded by a NERC Open CASE Award (NE/G011443/1) in collaboration with Reynolds International Ltd. Additional funding from the Postgraduate Discretionary Fund, Department of Geography, History and International Politics, Aberystwyth University, is also duly acknowledged. Photo Fig. 3B is credited to C. Souness. Past and present members of the Centre for Glaciology, Aberystwyth University, specifically John Balfour, Pippa Cowley, Sam Doyle, Heïdi Sevestre, Colin Souness and Ruth Taylor, and guides and porters from Summit Trekking, Kathmandu, are thanked for their support (both logistical and moral) on expeditions to the Khumbu Himal in 2010 and 2011, where investigation of a number of breached and extant moraine-dammed lake complexes helped considerably with the formulation and development of a number of key ideas and themes discussed in this paper. HR Wallingford and Halcrow are thanked for provision of academic software licences and guidance in the use of HR BREACH and ISIS 2D, respectively. Jürgen Herget and an anonymous reviewer are thanked for their constructive reviews, which helped to improve the clarity of the original manuscript.

References

Ageta, Y., Iwata, S., Yabuki, H., Naito, N., Sakai, A., Narama, C., Karma, 2000. Expansion of glacier lakes in recent decades in the Bhutan Himalayas. In: Nakawo, M., Raymond, C.F., Fountain, A. (Eds.), Debris-covered glaciers. Proceedings of a workshop held at Seattle, Washington, U.S.A, 264. IAHS Publication, Wallingford, pp. 165–175 (September).

Alean, J., 1985. Ice avalanches: some empirical information about their formation and reach. J. Glaciol. 31, 324–333.

Alho, P., Aaltonen, J., 2008. Comparing a 1D hydraulic model with a 2D hydraulic model for the simulation of extreme glacial outburst floods. Hydrol. Process. 22, 1537–1547.

Alho, P., Russell, A.J., Carrivick, J.L., Käykhö, J., 2005. Reconstruction of the largest Holocene jökulhlaup within Jökulsá á Fjöllum. Quat. Sci. Rev. 24, 2319–2334.

Allen, S., Owens, I., Sirguey, P., 2008. Satellite remote sensing procedures for glacial terrain analyses and hazard assessment in the Aoraki Mount Cook region, New Zealand. N. Z. J. Geol. Geophys. 51, 73–87.

Allen, S.K., Schneider, D., Owens, I.F., 2009. First approaches towards modelling glacial hazards in the Mount Cook region of New Zealand's Southern Alps. Nat. Hazards Earth Syst. Sci. 9, 481–499.

Armanini, A., Fraccarollo, L., Rosatti, G., 2008. Two-dimensional simulation of debris flows in erodible channels. Comput. Geosci. 35, 993–1006.

Ataie-Ashtiani, B., Nik-Khah, A., 2008. Impulsive waves caused by subaerial landslides. Environ. Fluid Mech. 8, 263–280.

Awal, R., Nakagawa, H., Fujita, M., Kawaike, K., Baba, Y., Zhang, H., 2010. Experimental study on Glacial Lake Outburst Floods due to wave overtopping and erosion of moraine dam. Ann. Disaster Prev. Res. Inst. 53, 583–594.

Bajracharya, S.R., Mool, P., 2009. Glaciers, glacial lakes and glacial lake outburst floods in the Mount Everest region, Nepal. Ann. Glaciol. 50, 81–86.

Bajracharya, B., Shrestha, A.B., Rajbhandar, L., 2007. Glacial Lake Outburst Floods in the Sagarmatha Region. Mt. Res. Dev. 27, 336–344.

Baker, V.R., 1988. Flood erosion. In: Baker, V.R., Kochel, R.C., Patton, P.C. (Eds.), Flood and Megaflood Processes and Deposits: Recent and Ancient Examples. Blackwell, Oxford, pp. 81–95.

Baker, V.R., 2000. Paleoflood hydrology and the estimation of extreme floods. In: Wohl, E. E. (Ed.), Inland Flood Hazards: Human, Riparian, and Aquatic Communities. Cambridge University Press, Cambridge, pp. 359–377.

Balmforth, N.J., von Hardenberg, J., Provenzale, A., Zammett, R., 2008. Dam breaking by wave-induced erosional incision. J. Geophys. Res. 113. http://dx.doi.org/10.1029/2007JF000756.

Balmforth, N.J., von Hardenberg, J., Zammett, R.J., 2009. Dam-breaking seiches. J. Fluid Mech. 628, 1–21.

Barré de St-Venant, A.J.C., 1871. Théorie et Equations Générales du Mouvement Non Permanent des Eaux Courantes. C. R. Séances Acad. Sci. 73, 147–154.

Batchelor, G.K., 1967. An Introduction to Fluid Dynamics. Cambridge University Press, Cambridge (615 pp.).

Benn, D.I., Owen, L.A., 2002. Himalayan glacial sedimentary environments: a framework for reconstructing and dating the former extent of glaciers in high mountains. Quat. Int. 97–98, 3–25.

Benn, D.I., Wiseman, S., Warren, C.R., 2000. Rapid growth of a supraglacial lake, Ngozumpa Glacier, Khumbu Himal, Nepal In: Nakawo, M., Raymond, C.F., Fountain, A. (Eds.), Debris-covered glaciers. Proceedings of a Workshop Held at Seattle, Washington, U.S.A., 264. IAHS Publication, Wallingford, pp. 177–185 (September).

Benn, D.I., Wiseman, S., Hands, K.A., 2001. Growth and drainage of supraglacial lakes on debris-mantled Ngozumpa Glacier, Khumbu Himal, Nepal. J. Glaciol. 47, 626–638.

Benn, D.I., Warren, C.R., Mottram, R.H., 2007. Calving processes and the dynamics of calving glaciers. Earth Sci. Rev. 82, 143–179.

Benn, D.I., Bolch, T., Hands, K., Gulley, J., Luckman, A., Nicholson, L.I., Quincey, D., Thompson, S., Toumi, R., Wiseman, S., 2012. Response of debris-covered glaciers in the Mount Everest region to recent warming and implications for outburst flood hazards. Earth Sci. Rev. 114, 156–174.

Bennett, G.L., Evans, D.J.A., 2012. Glacier retreat and landform production on an overdeepened glacier foreland: the debris-charged glacial landsystem at Kviárjökull, Iceland. Earth Surf. Process. Landf. 37, 1584–1602.

Bennett, M.R., Glasser, N.F., 2009. Glacial Geology: Ice Sheets and Landforms. Wiley-Blackwell, Chichester (385 pp.).

Beven, K.J., Binley, A., 1992. The future of distributed model: model calibration and uncertainty prediction. Hydrol. Process. 6, 279–298.

Björnsson, H., 2002. Subglacial lakes and jökulhlaups in Iceland. Glob. Planet. Chang. 35, 255–271.

Bremer, M., Sass, O., 2012. Combining airborne and terrestrial laser scanning for quantifying erosion and deposition by a debris flow event. Geomorphology 138, 49–60.

Di Baldassarre, G., Claps, P., 2011. A hydraulic study on the applicability of flood rating curves. Hydrol. Res. 42, 10–19.

Blazkova, S., Beven, K., 2004. Flood frequency estimation by continuous simulation of subcatchment rainfalls and discharges with the aim of improving dam safety assessment in a large basin in the Czech Republic. J. Hydrol. 292, 153–172.

Blown, I.G., Church, M., 1985. Catastrophic lake drainage within the Homathko River basin, British Columbia. Can. Geotech. J. 22, 551–563.

Bohorquez, P., Darby, S.E., 2008. The use of one- and two-dimensional hydraulic modelling to reconstruct a glacial outburst flood in a steep Alpine valley. J. Hydrol. 361, 240–261.

Boike, J., Yoshikawa, K., 2003. Mapping of periglacial geomorphology using kite/balloon aerial photography. Permafr. Periglac. Process. 14, 81–85.

Bolch, T., Buchroithner, M.F., Peters, J., Baessler, M., Bajracharya, S., 2008. Identification of glacier motion and potentially dangerous glacial lakes in the Mt. Everest region/Nepal using spaceborne imagery. Nat. Hazards Earth Syst. Sci. 8, 1329–1340.

Boniello, M.A., Calligaris, C., Lapasin, R., Zini, L., 2010. Rheological investigation and simulation of a debris-flow event in the Fella watershed. Nat. Hazards Earth Syst. Sci. 10, 989–997.

Breien, H., de Blasio, F.V., Elverhøi, A., Høeg, K., 2008. Erosion and morphology of a debris flow caused by a glacial lake outburst flood, Western Norway. Landslides 5, 271–280.

Broich, K., 2002. Determination of initial conditions for dam erosion due to overtopping and possible integration into a probabilistic design concept. Proceedings of the 2nd IMPACT workshop, Wallingford, UK (8 pp.).

Bursik, M., Martínez-Hackert, B., Delgado, H., Gonzalez-Huesca, A., 2003. A smoothed-particle hydrodynamic automaton of landform degradation by overland flow. Geomorphology 53, 25–44.

Cannata, M., Molinari, M.E., Marzocchi, R., 2012. Modeling of landslide-generated tsunamis with GRASS. Trans. GIS 16, 191–214.

Cao, Z., Pender, G., Wallis, S., Carling, P., 2004. Computational dam-break hydraulics over erodible sediment bed. J. Hydraul. Eng. ASCE 130, 689–703.

Cao, Z., Carling, P., 2002. Mathematical modelling of alluvial rivers: reality and myth. Part I: general overview. Water Marit. Eng. 154, 207–220.

Capart, H., 2013. Analytical solutions for gradual dam breaching and downstream river flooding. Water Resour. Res. 49, 1968–1987.

Capart, H., Young, D.L., 1998. Formation of a jump by the dam-break wave over a granular bed. J. Fluid Mech. 372, 165–187.

Capra, L., Macías, J.L., 2002. The cohesive Naranjo debris-flow deposit (10 km^3): a dam breakout flow derived from the Pleistocene debris-avalanche deposit of Nevado de Colima Volcano (México). J. Volcanol. Geotherm. Res. 117, 213–235.

Carrivick, J.L., Manville, V., Cronin, S.J., 2009. A fluid dynamics approach to modelling the 18th March 2007 lahar at Mt. Ruapehu, New Zealand. Bull. Volcanol. 71, 153–169.

Carrivick, J.L., Jones, R., Keevil, G., 2011. Experimental insights on geomorphological processes within dam break outburst floods. J. Hydrol. 408, 153–163.

Castellarin, A., Merz, R., Blöschl, G., 2009. Probabilistic envelope curves for extreme rainfall events. J. Hydrol. 378, 263–271.

Clague, J.J., Mathews, W.H., 1973. The magnitude of jökulhlaups. J. Glaciol. 12, 501–504.

Costa, J.E., 1985. Floods from dam failures. Us Geological Survey Open File Report 85-560 (54 pp.).

Carling, P.A., Glaister, M.S., 1987. Reconstruction of a flood resulting from a moraine-dam failure using geomorphological evidence and dam-break modeling. In: Mayer, L., Nash, D. (Eds.), Catastrophic Flooding. Allen and Unwin, Boston, pp. 182–200.

Carling, P., Villanueva, I., Herget, J., Wright, N., Borodavko, P., Morvan, H., 2009. Unsteady 1-D and 2-D hydraulic models with ice dam break for Quaternary megaflood, Altai Mountains, southern Siberia. Glob. Planet. Chang. 70, 24–34.

Carling, P.A., Villanueva, I., Herget, J., Wright, N., Borodavko, P., Morvan, H., 2010. Unsteady 1D and 2D hydraulic models with ice dam break for Quaternary megaflood, Altai Mountains, southern Siberia. Glob. Planet. Chang. 70, 24–34.

Carrivick, J.L., 2006. Application of 2D hydrodynamic modelling to high-magnitude outburst floods: an example from Kverkfjöll, Iceland. J. Hydrol. 321, 187–199.

Carrivick, J.L., 2007. Modelling coupled hydraulics and sediment transport of a high-magnitude flood and associated landscape change. Ann. Glaciol. 45, 143–154.

Carrivick, J.L., 2010. Dam break — Outburst flood propagation and transient hydraulics: a geosciences perspective. J. Hydrol. 380, 338–355.

Carrivick, J.L., Russell, A., Tweed, F.S., 2004. Geomorphological evidence for jökulhlaups from Kverkfjöll volcano, Iceland. Geomorphology 63, 81–102.

Carrivick, J.L., Manville, V., Graettinger, A., Cronin, S.J., 2010. Coupled fluid dynamics-sediment transport modelling of a Crater lake break-out lahar: Mt. Ruapehu, New Zealand. J. Hydrol. 388, 399–413.

Cenderelli, D.A., Wohl, E.E., 2001. Peak discharge estimates of glacial-lake outburst floods and "normal" climatic floods in the Mount Everest region, Nepal. Geomorphology 40, 57–90.

Cenderelli, D.A., Wohl, E.E., 2003. Flow hydraulics and geomorphic effects of glacial-lake outburst floods in the Mount Everest region, Nepal. Earth Surf. Process. Landf. 28, 385–407.

Centre for Energy Advancement through Technological Innovation (CEATI), 2012. Dam Safety Interest Group (DSIG). Available http://www.ceati.com/collaborative-programs/generation/dam-safety (Last accessed: 04 October 2012).

Chang, T.-J., Kao, H.-M., Chang, K.-H., Hsu, M.-H., 2011. Numerical simulation of shallow-water dam break flows in open channels using smoothed-particle hydrodynamics. J. Hydrol. 408, 78–90.

Chanson, H., 2004. The Hydraulics of Open Channel Flows: An Introduction, 2nd edition. Butterworth-Heinemann, Oxford (630 pp.).

Chen, Y.H., Simons, D.B., 1979. An experimental study of hydraulic and geomorphic changes in an alluvial channel induced by failure of a dam. Water Resour. Res. 15, 1183–1188.

Christen, M., Kowalski, J., Bartelt, P., 2010. RAMMS: numerical simulation of dense snow avalanches in three-dimensional terrain. Cold Reg. Sci. Technol. 63, 1–14.

Clague, J.J., Evans, S.G., 1992. A self-arresting moraine dam failure, St. Elias Mountains, British Columbia. Geol. Surv. Can. Pap. 92-1A, 185–188.

Clague, J.J., Evans, S.G., 1994. Formation and failure of natural dams in the Canadian Cordillera. Bull. Geol. Surv. Can. 464 (35 pp.).

Clague, J.J., Evans, S.G., 2000. A review of catastrophic drainage of moraine-dammed lakes in British Columbia. Quat. Sci. Rev. 19, 1763–1783.

Clague, J.J., Evans, S.G., Blown, I.G., 1985. A debris flow triggered by the breaching of a moraine-dammed lake, Klattasine Creek, British Columbia. Can. J. Earth Sci. 22, 1492–1502.

Cleary, P.W., Prakash, M., 2004. Discrete-element modelling and smoothed particle hydrodynamics: potential in the environmental sciences. Philos. Trans. Math. Phys. Eng. Sci. 362, 2003–2030.

Costa, J.E., 1983. Paleohydraulic reconstruction of flash-flood peaks from boulder deposits in the Colorado Front Range. Geol. Soc. Am. Bull. 94, 986–1004.

Costa, J.E., Schuster, R.L., 1988. The formation and failure of natural dams. Geol. Soc. Am. Bull. 100, 1054–1068.

Cristofano, E.A., 1965. Method of Computing Erosion Rate for Failure of Earthfill Dams. United States Bureau of Reclamation, Denver.

Dai, F.C., Lee, C.F., Deng, J.H., Tham, L.G., 2005. The 1786 earthquake-triggered landslide dam and subsequent dam-break flood on the Dadu River, southwestern China. Geomorphology 65, 205–221.

Delisle, G., Reynolds, J.M., Hanisch, J., Pokhrel, A.P., Pant, S., 2003. Lake Thulagi, Nepal: rapid landscape evolution in reaction to climate change. Ann. Geomorphol. 130, 1–9.

Desmet, P.J.J., Govers, G., 1996. Comparison of routing algorithms for digital elevation models and their implications for predicting ephemeral gullies. Int. J. Geogr. Inf. Sci. 10, 311–331.

Dunning, S.A., Rosser, N.J., Petley, D.N., Masser, C.R., 2006. Formation and failure of the Tsatichhu landslide dam, Bhutan. Landslides 3, 107–113.

Dunning, S.A., Large, A.R.G., Russell, A.J., Roberts, M.J., Duller, R., Woodward, J., Mériaux, A.-S., Tweed, F.S., Lim, M., 2013. The role of multiple glacier outburst floods in proglacial landscape evolution: the 2010 Eyjafjallajökull eruption, Iceland. Geology 41, 1123–1126.

Dupeyrat, L., Costard, F., Randriamazaoro, R., Gailhardis, E., Gautier, E., Fedorov, A., 2011. Effects of ice content on the thermal erosion of permafrost: implications for coastal and fluvial erosion. Permafr. Periglac. Process. 22, 179–187.

Emmer, A., Vilímek, V., 2013. Lake and breach hazard assessment for moraine-dammed lakes: an example from the Cordillera Blanca (Peru). Nat. Hazards Earth Syst. Sci. 13, 1551–1565.

Evans, S.F., 1986. The maximum discharge of outburst floods caused by the breaching of man-made and natural dams. Can. Geotech. J. 23, 385–387.

Evans, S.F., 1987. The breaching of moraine-dammed lakes in the southern Canadian Cordillera. Proceedings of the International Symposium on Engineering Geological Environment in Mountainous Areas, vol. 2. Science Press, Beijing, pp. 141–159.

Evans, S.G., Clague, J.J., 1994. Recent climatic change and catastrophic geomorphic processes in mountain environments. Geomorphology 10, 107–128.

Faeh, R., Mueller, R., Rousselot, P., Veprek, R., Vetsch, D., Volz, C., Vonwiller, L., Farshi, D., 2011. BASEMENT — Basic Simulation Environment for Computation of Environmental Flow and Natural Hazard Simulation. ETH Zurich (Available at: http://www.basement.ethz.ch).

Fell, R., Wan, C.F., Cyganiewicz, J., Foster, M., 2003. Time for development of internal erosion and piping in embankment dams. J. Geotech. Geoenviron. 129, 307–314.

Franz, K.J., Hogue, T.S., 2011. Evaluating uncertainty estimates in hydrologic models: borrowing measures from the forecast verification community. Hydrol. Earth Syst. Sci. 15, 3367–3382.

Fread, D.L., 1988a. The NWS DAMBRK Model: Theoretical Background/User Documentation. Office of Hydrology, National Weather Service, Silver Spring (328 pp.).

Fread, D.L., 1988b. BREACH: An Erosion Model for Earthen Dam Failures. (revised 1991) Office of Hydrology, National Weather Service, Silver Spring (35 pp.).

Fread, D.L., 1993. NWS FLDWAV model: the replacement of DAMBRK for dam-break flood prediction. Proceedings of the 10th Annual ASDSO Conference, pp. 177–184.

Fread, D.L., 1984. DAMBRK: The NWS dam-break flood forecasting model. Hydrologic Research Laboratory, Office of Hydrology, NWS, NOAA.

Frey, H., Haeberli, W., Linsbauer, A., Huggel, C., Paul, F., 2010. A multi-level strategy for anticipating future glacier lake formation and associated hazard potentials. Nat. Hazards Earth Syst. Sci. 10, 339–352.

Fritz, H.M., Hager, W.H., Minor, H.-E., 2003a. Landslide generated impulse waves. 1. Instantaneous flow fields. Exp. Fluids 35, 505–519.

Fritz, H.M., Hager, W.H., Minor, H.-E., 2003b. Landslide generated impulse waves. 2. Hydrodynamic impact craters. Exp. Fluids 35, 520–532.

Froehlich, D.C., 1995. Peak outflow from breached embankment dam. J. Water Resour. Plan. Manag. 121, 90–97.

Gatto, L.W., 1995. Soil Freeze–thaw Effects on Bank Erodibility and Stability. Special report 95-24. Cold Regions Research and Engineering Laboratory, Hanover.

Gardelle, J., Arnaud, Y., Berthier, E., 2001. Contrasted evolution of glacial lakes along the Hindu Kush Himalaya mountain range between 1990 and 2009. Glob. Planet. Chang. 75, 47–55.

Grabs, W.E., Hanisch, J., 1993. Objectives and prevention methods for Glacier Lake Outburst Floods (GLOFs). In: Young, G.J. (Ed.), Snow and Glacier Hydrology. IAHS Publ, No. 218, pp. 341–352.

Grove, J.M., 2004. Little Ice Ages: Ancient and Modern, second edition. Routledge, London (760 pp.).

Guðmundsson, M.T., Björnsson, H., Pálsson, F., 1995. Changes in jökulhlaup sizes in Grímsvötn, Vatnajökull, Iceland, 1934-1991, deduced from in situ measurements of subglacial lake volume. J. Glaciol. 41, 263–272.

Haeberli, W., 1983. Frequency and characteristics of glacier floods in the Swiss Alps. Ann. Glaciol. 4, 85–90.

Haeberli, W., Kääb, A., Mühll, D.V., Teysseire, P., 2001. Prevention of outburst floods from periglacial lakes at Grubengletscher, Valais, Swiss Alps. J. Glaciol. 47, 111–122.

Hagen, V.K., 1982. Re-evaluation of design floods and dam safety. Proceedings of the 14th Congress of International Commission on Large Dams. International Commission on Large Dams, Paris, France, Rio de Janeiro, Brazil.

Hall, J.W., Tarantola, S., Bates, P.D., Horritt, M.S., 2005. Distributed sensitivity analysis of flood inundation model calibration. J. Hydraul. Eng. ASCE 131, 117–126.

Hambrey, M.J., Quincey, D.J., Glasser, N.F., Reynolds, J.M., Richardson, S.D., Clemmens, S., 2009. Sedimentological, geomorphological and dynamic context of debris-mantled glaciers, Mount Everest (Sagarmatha) region, Nepal. Quat. Sci. Rev. 27, 2361–2389.

Hanisch, J., Delisle, G., Pokhrel, A.P., Dixit, A.M., Reynolds, J.M., Grabs, W.E., 1998. The Thulagi glacier lake, Manaslu Himal, Nepal: hazard assessment of a potential outburst. Proeedings of the Eighth International IAEG Congress, 21-25 September 1998, Vancouver, Canada, pp. 2209–2215.

Hanson, G.J., Cook, K.R., 2004. Apparatus, test procedures, and analytical methods to measure soil erodibility *in situ*. Appl. Eng. Agric. 20, 455–462.

Hanson, G.J., Hunt, S.L., 2007. Lessons learned using laboratory JET method to measure soil erodibility of compacted soils. Appl. Eng. Agric. 23, 305–312.

Harris, G.W., Wagner, D.A., 1967. Outflow from Breached Earth Dams. University of Utah, Logan.

Harrison, S., Glasser, N.F., Winchester, V., Haresign, E., Warren, C., Jansson, K., 2006. A glacial lake outburst flood associated with recent mountain glacier retreat, Patagonian Andes. The Holocene 16, 611–620.

Hervouet, J.-M., 2007. *Hydrodynamics of Free Surface Flows: Modelling with the Finite Element Method*. Wiley Blackwell, Chichester (360 pp.).

Hewitt, K., 1982. Natural dams and outburst floods of the Karakoram Himalaya. In: Glen, J. W. (Ed.), Hydrological Aspects of Alpine and High-Mountain Areas: Proceedings of the Exeter IAHS Symposium, July 1982. IAHS Publ, No. 138, pp. 259–269.

Hewitt, K., Liu, J., 2010. Ice-dammed lakes and outburst floods, Karakoram Himalaya: historical perspectives on emerging threates. Phys. Geogr. 31, 528–551.

Hochstein, M.P., Claridge, D., Henrys, S.A., Pyne, A., Nobes, D.C., Leary, S.F., 1995. Downwasting of the Tasman Glacier, South Island, New Zealand: changes in the terminus region between 1971 and 1993. N. Z. J. Geol. Geophys. 38, 1–16.

Hogg, A.J., Pritchard, D., 2004. The effects of hydraulic resistance on dam-break and other shallow inertial flows. J. Fluid Mech. 501, 179–212.

Horritt, M.S., Bates, P.D., 2002. Evaluation of 1D and 2D numerical models for predicting river flood inundation. J. Hydrol. 268, 87–99.

Huang, Y., Dai, Z., Zhang, W., Chen, Z., 2011. Visual simulation of landslide fluidized movement based on smoothed particle hydrodynamics. Nat. Hazards 59, 1225–1238.

Huang, Y., Zhang, W., Xu, Q., Xie, P., Hao, L., 2012. Run-out analysis of flow like landslides triggered by the Ms 8.0 2008 Wenchuan earthquake using smoothed particle hydrodynamics. Landslides 9, 275–283.

Hubbard, B., Heald, A., Reynolds, J.M., Quincey, D.J., Richardson, S.D., Luyo, M.Z., Portilla, N.S., Hambrey, M.J., 2005. Impact of a rock avalanche on a moraine-dammed proglacial lake: Laguna Safuna Alta, Cordillera Blanca, Peru. Earth Surf. Process. Landf. 30, 1251–1264.

Hubbard, B.E., Sheridan, M.F., Carrasco-Núñez, G., Díaz-Castellón, R., Rodríguez, S.R., 2007. Comparative lahar hazard mapping at Volcan Citlaltépetl, Mexico using SRTM, ASTER and DTED-1 digital topographic data. J. Volcanol. Geotherm. Res. 160, 99–124.

Huggel, C., Kääb, A., Haeberli, W., Teysseire, P., Paul, F., 2002a. Remote sensing based assessment of hazards from glacier lake outbursts: a case study in the Swiss Alps. Can. Geotech. J. 39, 316–330.

Huggel, C., Haeberli, W., Kääb, A., Hoelzle, M., Ayros, E., Portocarrero, C., 2002b. Assessment of glacier hazards and glacier runoff for different climate scenarios based on remote sensing data: a case study for a hydropower plant in the Peruvian Andres. EARSeL eProc. 2, 22–33.

Huggel, C., Kääb, A., Haeberli, W., Krummenacher, B., 2003. Regional-scale GIS-models for assessment of hazards from glacier lake outbursts: evaluation and application in the Swiss Alps. Nat. Hazards Earth Syst. Sci. 3, 647–662.

Huggel, C., Haeberli, W., Kääb, A., Bieri, D., Richardson, S., 2004. An assessment procedure for glacial hazards in the Swiss Alps. Can. Geotech. J. 41, 1068–1083.

Huggel, C., Zgraggen-Oswald, S., Haeberli, W., Kääb, A., Polkvoj, A., Galushkin, I., Evans, S. G., 2005. The 2002 rock/ice avalanche at Kolka/Karmadon, Russian Caucasus: assessment of extraordinary avalanche formation and mobility, and application of QuickBird satellite imagery. Nat. Hazards Earth Syst. Sci. 5, 173–187.

Huggel, C., Kääb, A., Salzmann, N., 2006. Evaluation of QuickBird and IKONOS imagery for assessment of high-mountain hazards. EARSeL eProc. 5, 51–62.

Huggel, C., Schneider, D., Miranda, P.J., Granados, H.D., Kääb, A., 2008. Evaluation of ASTER and SRTM DEM data for lahar modeling: a case study on lahars from Popocatépetl Volcano, Mexico. J. Volcanol. Geotherm. Res. 170, 99–110.

Hungr, O., 1995. A model for the runout analysis of rapid flow slides, debris flows, and avalanches. Can. Geotech. J. 32, 610–623.

IPCC, 2013. Climate Change 2013: The Scientific Basis. Working Group I Contribution to the IPCC Fifth Assessment Report (127 pp. Available: http://www.ipcc.ch/report/ar5/wg1/#.UrcaEvRdWSp).

Irvine-Fynn, T.D.L., Barrand, N.E., Porter, P.R., Hodson, A.J., Murray, T., 2011. Recent High-Arctic glacial sediment redistribution: a process perspective using airborne lidar. Geomorphology 125, 27–39.

Iverson, R.M., 1997. The physics of debris flows. Rev. Geophys. 35, 245–296.

Iverson, R.M., Reid, M.E., Logan, M., LaHusen, R.G., Godt, J.W., Griswold, J.P., 2011. Positive feedback and momentum growth during debris-flow entrainment of wet bed sediment. Nat. Geosci. 4, 116–121.

Iwata, S., Ageta, Y., Naito, N., Sakai, A., Narama, C., Karma, 2002. Glacial lakes and their outburst flood assessment in the Bhutan Himalaya. Glob. Environ. Res. 6, 3–17.

Janský, B., Engel, Z., Šobr, M., Beneš, V., Špaček, K., Yerokhin, S., 2009. The evolution of Petrov lake and moraine dam rupture risk (Tien-Shan, Kyrgyzstan). Nat. Hazards 50, 83–96.

Janský, B., Šobr, M., Engel, Z., 2010. Outburst flood hazard: case studies from the Tien-Shan Mountains, Kyrgyzstan. Limnologica 40, 358–364.

Kääb, A., Huggel, C., Fischer, L., Guex, S., Paul, F., Roer, I., Salzmann, N., Schlaefli, S., Schmutz, K., Schneider, D., Strozzi, T., Weidmann, Y., 2005. Remote sensing of glacier- and permafrost-related hazards in high mountains: an overview. Nat. Hazards Earth Syst. Sci. 5, 527–554.

Kääb, A., Huggel, C., Paul, F., Wessels, R., Raup, B., Kieffer, H., Kargel, J., 2002. Glacier monitoring from ASTER imagery: accuracy and implications. EARSeL eProc. 2, 43–52.

Kao, H.-M., Chang, T.-J., 2012. Numerical modelling of dambreak-induced flood and inundation using smoothed particle hydrodynamics. J. Hydrol. 448–449, 232–244.

Kershaw, J.A., Clague, J.J., Evans, S.G., 2005. Geomorphic and sedimentological signature of a two-phase outburst flood from moraine-dammed Queen Bess Lake, British Columbia, Canada. Earth Surf. Process. Landf. 30, 1–25.

Kidson, R.L., Richards, K.S., Carling, P.A., 2006. Hydraulic model calibration for extreme floods in bedrock-confined channels: Case study from northern Thailand. Hydrol. Process. 20, 329–344.

Kirkpatrick, G.W., 1977. Evaluation guidelines for spillway adequacy. Proceedings of the American Society of Civil Engineers Engineering Foundation Conference 1977, Pacific Grove, California, pp. 395–414.

Komori, J., 2008. Recent expansions of glacial lakes in the Bhutan Himalayas. Quat. Int. 184, 177–186.

Korup, O., Tweed, F., 2007. Ice, moraine, and landslide dams in mountainous terrain. Quat. Sci. Rev. 26, 3406–3422.

Kuczera, G., Parent, E., 1998. Monte Carlo assessment of parameter uncertainty in conceptual catchment models: the Metropolis algorithm. J. Hydrol. 211, 69–85.

Laigle, D., Lachamp, P., Naaim, M., 2007. SPH-based numerical investigation of mudflow and other complex fluid flow interactions with structures. Comput. Geosci. 11, 297–306.

Lamb, R., Beven, K., Myrabo, S., 1998. Use of spatially distributed water table observations to constrain uncertainty in a rainfall-runoff model. Adv. Water Resour. 22, 305–317.

Lancaster, S.T., Hayes, S.K., Grant, G.E., 2003. Effects of wood on debris flow runout in small mountain watersheds. Water Resour. Res. 39. http://dx.doi.org/10.1029/2001WR001227.

Langston, G., Bentley, L.R., Hayashi, M., McClymont, A., Pidlisecky, A., 2011. Internal structure and hydrological functions of an alpine proglacial moraine. Hydrol. Process. 25, 2967–2982.

Laurent, G., Soares-Frazao, S., Zech, Y., 2011. Dam-break flow on mobile bed in abruptly widening channel: experimental data. ASCE J. Hydraul. Res. 49, 367–371.

Leal, J.G.A.B., Ferreira, R.M.L., Cardoso, A.H., 2009. Maximum level and time to peak of dam-break waves on mobile horizontal bed. J. Hydraul. Eng. ASCE 135, 995–999.

Lejot, J., Delacourt, C., Piégay, H., Fournier, T., Trémélo, M.-L., Allemand, P., 2007. Very high spatial resolution imagery for channel bathymetry and topography from an unmanned mapping controlled platform. Earth Surf. Process. Landf. 32, 1705–1725.

Liang, C., Mackay, D.S., 2000. A general model of watershed extraction and representation using globally optimal flow paths and up-slope contributing areas. Int. J. Geogr. Inf. Sci. 14, 337–358.

Liao, C.B., Wu, M.S., Liang, S.J., 2007. Numerical simulation of a dam break for an actual river terrain environment. Hydrol. Process. 21, 447–460.

Lick, W., McNeil, J., 2001. Effects of sediment bulk properties on erosion rates. Sci. Total Environ. 266, 41–48.

Liu, G.R., Liu, M.B., 2010. Smoothed particle hydrodynamics (SPH): an overview and recent developments. Arch. Comput. Meth. Eng. 17, 25–76.

Lliboutry, L., Arnao, B.M., Pautre, A., Schneider, B., 1997a. Glaciological problems set by the control of dangerous lakes in Cordillera Blanca, Peru I: Historical failures of morainic dams, their causes and prevention. J. Glaciol. 18, 239–254.

Lliboutry, L., Arnao, B.M., Schneider, B., 1977b. Glaciological problems set by the control of dangerous lakes in Cordillera Blanca, Peru III: Study of moraines and mass balances at Safuna. J. Glaciol. 18, 275–290.

Macdonald, T.C., Langridge-Monopolis, J., 1984. Breaching characteristics of dam failures. J. Hydraul. Eng. 110, 567–586.

Manville, V., 2004. Paleohydraulic analysis of the 1953 Tangiwai lahar: New Zealand's worst volcanic disaster. Acta Vulcanol. 16, 137–152.

Margreth, S., Funk, M., 1999. Hazard mapping for ice and combined snow/ice avalanches: two case studies from the Swiss and Italian Alps. Cold Reg. Sci. Technol. 30, 159–173.

Marren, P.M., 2005. Magnitude and frequency in proglacial rivers: a geomorphological and sedimentological perspective. Earth Sci. Rev. 70, 203–251.

Mayo, L.R., 1989. Advance of Hubbard Glacier and closure of Russell Fiord, Alaska: environmental effects and hazards in the Yakutat area. USGS Circ. 1016, 4–16.

Mergili, M., Schneider, J.F., 2011. Regional-scale analysis of lake outburst hazards in the southwestern pamir, Tajikistan, based on remote sensing and GIS. Nat. Hazards Earth Syst. Sci. 11, 1447–1462.

Mergili, M., Schratz, K., Ostermann, A., Fellin, W., 2012. Physically-bsed modelling of granular flows with Open Source GIS. Nat. Hazards Earth Syst. Sci. 12, 187–200.

McKillop, R.J., Clague, J.J., 2007. Statistical, remote sensing-based approach for estimating the probability of catastrophic drainage from moraine-dammed lakes in southwestern British Columbia. Glob. Planet. Chang. 56, 153–171.

Meon, G., Schwarz, W., 1993. Estimation of Glacier Lake Outburst Flood and its impact on a hydro project in Nepal. In: Young, G.J. (Ed.), Snow and Glacier Hydrology. IAHS Publication, No. 209, pp. 331–340.

Mohamed, M.A.A., Samuels, P.G., Morris, M.W., Ghataora, G.S., 2002. Improving the accuracy of prediction of breach formation through embankment dams and flood embankments. In: Bousmar, D., Zech, Y. (Eds.), River Flow 2002: 1st International Conference on Fluvial Hydraulics, Louvain-la-Neuve, Belgium, September 3–6 (Online proceedings. Available: http://sites.uclouvain.be/gce/~hydraulique/riverflow/proc/toc.html#C4).

Mool, P., Bajracharya, S., Joshi, S.P., 2001. Inventory of glaciers, glacial lakes, and glacial lake outburst floods: monitoring and early warning systems in the Hindu–Kush–Himalayan region (Kathmandu: ICIMOD and Bangkok: UNEP/RRC-AP).

Moore, J.R., Boleve, A., Sanders, J.W., Glaser, S.D., 2011. Self-potential investigation of moraine dam seepage. J. Appl. Geophys. 74, 277–286.

Morris, M.W., Hassan, M., Vaskinn, K.A., 2007. Breach formation: field test and laboratory experiments. J. Hydraul. Res. 45, 9–17.

Morris, M.W., Hanson, G., Hassan, M., 2008. Improving the accuracy of breach modelling: why are we not progressing faster? J. Flood Risk Manage. 1, 150–161.

Morris, M., Hassan, M., Kortenhaus, A., Visser, P., 2009a. Breaching Processes: A state of the art review. FLOOD site Project Report, T06-06-03. 70pp.

Morris, M.W., Hassan, M., Kortenhaus, A., Geisenhainer, P., Visser, P.J., Zhu, Y., 2009b. Modelling breach initiation and growth. In: Samuels, P., Huntington, S., Allsop, W., Harrop, J. (Eds.), Flood Risk Management: Research and Practice. Routledge, London, pp. 581–591.

Motyka, R.J., Truffer, M., 2007. Hubbard Glacier, Alaska: 2002 closure of Russell Fjord and implications for future dams. J. Geophys. Res. 112 (F2). http://dx.doi.org/10.1029/2006JF000475 (F02004).

Muller, D.R., 1995. Auflaufen and Uverschwappen von Impulswellen an Talsperren. VAW-ETH, Zurich (Mitt. Nr. 137).

Niethammer, U., James, M.R., Rothmund, S., Travelletti, J., Joswig, W., 2012. UAV-based remote sensing of the Super Sauze landslide: evaluation and results. Eng. Geol. 128, 2–11.

Nsom, B., 2002. Horizontal viscous dam-break flow: experiments and theory. J. Hydraul. Eng. ASCE 128, 543–546.

O'Brien, J.S., 2003. Reasonable assumptions in routing a dam break flood. In: Rickenmann, D., Chen, C. (Eds.), Debris-flow Hazards Mitigation: Mechanics, Prediction and Assessment. Proceedings of the Third International DFHM Conference, Davos Switzerland, September 10–12, 2003. Millpress, Rotterdam, pp. 683–693.

O'Callaghan, J.F., Mark, D.M., 1984. The extraction of drainage networks from digital elevation data. Comput. Vis. Graph. Image Proc. 28, 323–344.

O'Connor, J.E., Hardison, J.H., Costa, J.E., 1994. Breaching of lakes impounded by Neoglacial moraines in the Cascade Range, Oregon and Washington. Geol. Soc. Am. Abstr. Programs 26, A-218–A-219.

O'Connor, J.E., Hardison, J.H., Costa, J.E., 2001. Debris flows from failures of Neoglacial-age moraines in the Three Sisters and Mount Jefferson wilderness areas, Oregon. US Geol. Surv. Prof. Pap. 1606.

Osti, R., Egashira, S., 2009. Hydrodynamic characteristics of the Tam Pokhari Glacial Lake outburst flood in the Mt. Everest region, Nepal. Hydrol. Process. 23, 2943–2955.

Osti, R., Bhattarai, T.N., Miyake, K., 2011. Causes of catastrophic failure of Tam Pokhari moraine dam in the Mt. Everest region. Nat. Hazards 58, 1209–1223.

Pant, S.R., Reynolds, J.M., 2000. Application of electrical imaging techniques for the investigation of natural dams: an example from the Thulagi Glacier Lake, Nepal. J. Nepal Geol. Soc. 22, 211–218.

Pappenberger, F., Beven, K.J., Hunter, N.M., Bates, P.D., Gouweleeuw, B.T., Thielen, J., de Roo, A.P.J., 2005. Cascading model uncertainty from medium range weather forecasts (10 days) through a rainfall-runoff model to flood inundation predictions within the European Flood Forecasting System (EFFS). Hydrol. Earth Syst. Sci. 9, 381–393.

Pappenberger, F., Matgen, P., Beven, K.J., Henry, J.-B., Pfister, L., Fraipont de, P., 2006. Influence of uncertain boundary conditions and model structure on flood inundation predictions. Adv. Water Resour. 29, 1430–1449.

Pastor, M., Herreros, I., Fernández, M., Mira, B., Haddad, B., Quecedo, M., González, E., Alvarez-Cedrón, C., Drempetic, V., 2009. Modelling of fast catastrophic landslides and impulse waves induced by them in fjords, lakes and reservoirs. Eng. Geol. 109, 124–134.

Pastor, M., Herreros, I., Fernández Merodo, J.A., Mira, P., Haddad, B., Quecedo, m., González, E., Alvarez-Cedrón, Drempetic, V., 2009. Modelling of fast catastrophic landslides and impulse waves induced by them in fjords, lakes and reservoirs. Eng. Geol. 109, 124–134.

Pierce, M.W., Thornton, C.I., Abt, S.R., 2010. Predicting peak outflow from breached embankment dams. J. Hydrol. Eng. ASCE 15, 338–349.

Pitman, E.B., Patra, A.K., Kumar, D., Nishimura, K., Komori, J., 2013. Two phase simulation of glacier lake outburst flows. J. Comput. Sci. 4, 71–79.

Procter, J., Cronin, S.J., Fuller, I.C., Lube, G., Manville, V., 2010. Quantifying the geomorphic impacts of a lake-breakout lahar, Mount Ruapehu, New Zealand. Geology 38, 67–70.

Quincey, D.J., Lucas, R.M., Richardson, S.D., Glasser, N.F., Hambrey, M.J., Reynolds, J.M., 2005. Optical remote sensing techniques in high-mountain environments: application to glacial hazards. Prog. Phys. Geogr. 29, 475–505.

Quincey, D.J., Richardson, S.D., Luckman, A., Lucas, R.M., Reynolds, J.M., Hambrey, M.J., Glasser, N.F., 2007. Early recognition of glacial lake hazards in the Himalaya using remote sensing datasets. Glob. Planet. Chang. 56, 137–152.

Rana, B., Shrestha, A.B., Reynolds, J.M., Aryal, R., Pokhrel, A.P., Budhathoki, K.P., 2000. Hazard assessment of the Tsho Rolpa Glacier Lake and ongoing remediation measures. J. Nepal Geol. Soc. 22, 563–570.

Reynolds, J.M., 1981. Lake on George VI Ice Shelf, Antarctica. Polar Rec. 20, 425–432.

Reynolds, J.M., 1992. The identification and mitigation of glacier-related hazards: examples from the Cordillera Blanca, Peru. In: McCall, G.J.H., Laming, D.C.J., Scott, S. (Eds.), Geohazards. Chapman and Hall, London, pp. 143–157.

Reynolds, J.M., 1998a. Managing the risks of glacial flooding at hydro plants. Hydro Rev. Worldw. 6, 18–22.

Reynolds, J.M., 1998b. High altitude glacial lake hazard assessment and mitigation: a Himalayan perspective. In: Maund, J., Eddleston, M. (Eds.), Geohazards in Engineering Geology. Geological Society Engineering Group Special Publication, No. 15, pp. 25–34.

Reynolds, J.M., 2000. On the formation of supraglacial lakes on debris-covered glaciers. In: Nakawo, M., Raymond, C.F., Fountain, A. (Eds.), Debris-covered Glaciers. Proceedings of a workshop held at Seattle, Washington, U.S.A., September, 264. IAHS Publication, Wallingford, pp. 153–161.

Reynolds, J.M., 2006. The role of geophysics in glacial hazard assessment. First Break 24, 61–66.

Reynolds, J.M., 2011. An Introduction to Applied and Environmental Geophysics, 2nd edition. John Wiley & Sons Ltd, Chichester (712 pp.).

Reynolds Geo-Sciences Ltd, 2003. Development of glacial hazard and risk minimisation protocols in rural environments: guidelines for the management of glacial hazards and risks. Report R7816 Reynolds Geo-Sciences Ltd, Mold, UK (Available online: http://www.reynolds-international.co.uk/dfid).

Reynolds, J.M., Dolecki, A., Portocarrero, C., 1998. The construction of a drainage tunnel as part of glacial lake hazard mitigation at Hualcán, Cordillera Blanca, Peru. In: Maund, J., Eddleston, M. (Eds.), Geohazards in Engineering Geology. Geological Society of Engineering Group Special Publication, No. 15, pp. 41–48.

Richards, K., Bithell, M., Dove, M., Hodge, R., 2004. Discrete-element modelling: methods and applications in the environmental sciences. Philos. Trans. Math. Phys. Eng. Sci. 362, 1797–1816.

Richardson, S.D., Reynolds, J.M., 2000a. An overview of glacial hazards in the Himalayas. Quat. Int. 65 (66), 31–47.

Richardson, S.D., Reynolds, J.M., 2000b. Degradation of ice-cored moraine dams: implications for hazard development. In: Nakawo, M., Raymond, C.F., Fountain, A. (Eds.), Debris-covered Glaciers. Proceedings of a workshop held at Seattle, Washington, U.S.A., September, 264. IAHS Publication, Wallingford, pp. 187–198.

Rickenmann, D., 1999. Empirical relationships for debris flows. Nat. Hazards 19, 47–77.

Rickenmann, D., Laigle, D., McArdell, B.W., Hübl, J., 2006. Comparison of 2D debris-flow simulation models with field events. Comput. Geosci. 10, 241–264.

Riggs, H.C., 1976. A simplified slope-area method for estimating flood discharges in natural channels. US Geol. Surv. J. Res. 4, 285–291.

Risley, J., Walder, J., Delinger, R., 2006. Usoi dam wave overtopping and flood routing in the Bartang and Panj Rivers, Tajikistan. USGS Water-Resources Investigations Report 03-4004.

Ritchie, J.B., Lingle, C.S., Motyka, R.J., Truffer, M., 2008. Seasonal fluctuations in the advance of a tidewater glacier and potential causes: Hubbard Glacier, Alaska, USA. J. Glaciol. 54, 401–411.

Roberts, M., Tweed, F., Russell, A., Knudsen, O., Harris, T., 2003. Hydrologic and geomorphic effects of temporary ice-dammed lake formation during Jökulhlaups. Earth Surf. Process. Landf. 28, 723–737.

Robertson, C., Benn, D.I., Brook, M.S., Fuller, I.C., Holt, K.A., 2012. Subaqueous calving margin morphology at Mueller, Hooker and Tasman glaciers in Aoraki/Mount Cook National Park, New Zealand. J. Glaciol. 58, 1037–1046.

Röhl, K., 2006. Thermo-erosional notch development at fresh-water-calving Tasman Glacier, New Zealand. J. Glaciol. 52, 203–213.

Röhl, K., 2008. Characteristics and evolution of supraglacial ponds on debris-covered Tasman Glacier, New Zealand. J. Glaciol. 54, 867–880.

Rudoy, A.N., 2002. Glacier-dammed lakes and geological work of glacial superfloods in the Late Pleistocene, Southern Siberia, Altai Mountains. Quat. Int. 87, 119–140.

Rushmer, E.L., 2007. Physical-scale modelling of jökulhlaups (glacial outburs floods) with contrasting hydrograph shapes. Earth Surf. Process. Landf. 32, 954–963.

Russell, A.J., Knudsen, Ó., Maizels, J.K., Marren, P.M., 1997. Controls on the geomorphological impact of the November 1996 jökulhlaup, Skeiðarársandur, Iceland. In Supplementi di Geogfia Fisica e Dinamica Quaternaria III (abstracts of the Fourth International Conference on Geomorphology), Bologna, International Association of Geomorphologists, pp. 335–336.

Russell, A., Tweed, F.S., Roberts, M.J., Harris, T.D., Gudmundsson, M.T., Knudsen, O., Marren, P.M., 2010. An unusual jökulhlaup resulting from subglacial volcanism, Sólheimajökull, Iceland. Quat. Sci. Rev. 29, 1363–1381.

Sailer, R., Fellin, W., Fromm, R., Jörg, P., Rammer, L., Sampl, P., Schaffhauser, A., 2008. Snow avalanche mass-balance calculation and simulation-model verification. Ann. Glaciol. 48, 183–192.

Sakai, A., Fujita, K., 2010. Formation conditions of supraglacial lakes on debris-covered glaciers in the Himalaya. J. Glaciol. 56, 177–181.

Sakai, A., Chikita, K., Yamada, T., 2000. Expansion of a moraine-dammed glacial lake, Tsho Rolpa, in Rolwaling Himal, Nepal Himalaya. Limnol. Oceanogr. 45, 1401–1408.

Sakai, A., Nishimura, K., Kadota, T., Takeuchi, N., 2009. Onset of calving at supraglacial lakes on debris-covered glaciers of the Nepal Himalaya. J. Glaciol. 55, 909–917.

Salzmann, N., Kääb, A., Huggel, C., Allgöwer, B., Haeberli, W., 2004. Assessment of the hazard potential of ice avalanches using remote sensing and GIS-modelling. Nor. J. Geogr. 58, 74–84.

Sampl, P., Zwinger, T., 2004. Avalanche simulation with SAMOS. Ann. Glaciol. 38, 393–398.

Sanders, B.F., 2007. Evaluation of on-line DEMs for flood inundation modelling. Adv. Water Resour. 30, 1831–1843.
Sawagaki, T., Lamsal, D., Byers, A., Watanabe, T., 2013. Changes in surface morphology and glacial lake development of Chamlang South Glacier in the Eastern Nepal Himalaya since 1964. Global Environ. Res. 16, 83–94.
Schneider, D., Bartelt, P., Caplan-Auerbach, J., Christen, M., Huggel, C., McArdell, B.W., 2010. Insights into rock-ice avalanche dynamics by combined analysis of seismic recordings and a numerical avalanche model. J. Geophys. Res. 115. http://dx.doi.org/10.1029/2010JF001734 (F04026).
Shrestha, A.B., Eriksson, M., Mool, P., Ghimire, P., Mishra, B., Khanal, N.R., 2010. Glacial lake outburst flood risk assessment of Sun Koshi basin, Nepal. Geomatics Nat. Hazards Risk 1, 157–169.
Simpson, G., Castelltort, S., 2006. Coupled model of surface water flow, sediment transport and morphological evolution. Comput. Geosci. 32, 1600–1614.
Singh, K.P., Snorrason, A., 1982. Sensitivity of outflow peaks and flood stages to the selection of dam breach parameters and simulation models. SWS Contract Report No. 288, Illinois Department of Energy and Natural Resources, State Water Survey Division, University of Illinois (179 pp.).
Singh, K.P., Snorrason, A., 1984. Sensitivity of outflow peaks and flood stages to the selection of dam breach parameters and simulation models. J. Hydrol. 68, 295–310.
Smith, M., Chandler, J., Rose, J., 2009. High spatial resolution data acquisition for the geosciences: kite aerial photography. Earth Surf. Process. Landf. 34, 155–161.
Stansby, P.K., Chegini, A., Barnes, T.C.D., 1998. The initial stages of dam-break flow. J. Fluid Mech. 374, 407–424.
Stoltz, A., Huggel, C., 2008. Debris flows in the Swiss National Park: the influence of different flow models and varying DEM grid size on modeling results. Landslides 5, 311–319.
Strasser, M., Schindler, C., Anselmetti, F.S., 2008. Late Pleistocene earthquake-triggered moraine dam failure and outburst of Lake Zurich, Switzerland. J. Geophys. Res. 113 (F02003).
Synolakis, C.E., 1987. The runup of solitary waves. J. Fluid Mech. 185, 523–545.
Tarboton, D.G., 1997. A new method for the determination of flow directions and upslope areas in grid digital elevation models. Water Resour. Res. 33, 309–319.
Temple, D.M., Hanson, G.J., Neilsen, M.L., Cook, K.R., 2005. Simplified breach analysis model for homogeneous embankments: Part I, Background and model components. Proceedings of the 2005 US Society of Dams Annual Meeting and Conference, Salt Lake City, Utah, pp. 151–161.
Thompson, S.S., Benn, D.I., Dennis, K., Luckman, A., 2012a. A rapidly-growing moraine-dammed glacial lake on Ngozumpa Glacier, Nepal. Geomorphology 145–146, 1–11.
Thompson, S., Kulessa, B., Luckman, A., 2012b. Integrated electrical resistivity tomography (ERT) and self-potential (SP) techniques for assessing hydrological processes within glacial lake moraine dams. J. Glaciol. 58, 1–10.
Tweed, F.S., Russell, A.J., 1999. Controls on the formation and sudden drainage of glacier-impounded lakes: implications for jökulhlaup characteristics. Prog. Phys. Geogr. 23, 79–110.
Thornton, C.I., Pierce, M.W., Abt, S.R., 2011. Enhanced predictions for peak outflow from breached embankment dams. J. Hydrol. Eng. ASCE 16, 81–88.
US Army Corps of Engineers (USACE), 2010. HEC-RAS River Analysis System (Version 4.1). Hydrologic Engineering Center, Davis (790 pp.).
US Bureau of Reclamation, 1982. Guidelines for Defining Inundated Areas Downstream from Bureau of Reclamation Dams. Reclamation Planning Instruction No. 82-11 (June 15, 1982. 22 pp.).
US Soil Conservation Service, 1981. Simplified Dam-Breach Routing Procedure. Technical Release No. 66 (December 1981. 39 pp.).
Vaskinn, K.A., Lövoll, A., Hoëg, K., Morris, M., Hanson, G.J., Hassan, M.A., 2004. Physical modeling of breach formation: large scale field tests. Dam Safety 2004, Proceedings of the Association of State Dam Safety Officials, September 2004, Phoenix, Arizona (16 pp.).
Vericat, D., Brasington, J., Wheaton, J., Cowie, M., 2009. Accuracy assessment of aerial photographs acquired using lighter-than-air blimps: low cost tools for mapping river corridors. River Res. Appl. 25, 985–1000.
Vuichard, D., Zimmerman, M., 1986. The Langmoche flash-flood, Khumbu Himal, Nepal. Mt. Res. Dev. 6, 90–94.
Vuichard, D., Zimmerman, M., 1987. The 1985 catastrophic drainage of a moraine-dammed lake, Khumbu Himal, Nepal: cause and consequences. Mt. Res. Dev. 7, 91–110.
Wahl, T.L., 1997. Predicting embankment dam breach parameters: A needs assessment. XXVIIth IAHR Congress, San Francisco, California (August 10-15, 1997. 7 pp.).
Wahl, T., 1998. Prediction of Embankment Dam Breach Parameters: A Literature Review and Needs Assessment. Water Resources Research Laboratory, Denver (67 pp.).
Wahl, T., 2004. Uncertainty of predictions of embankment dam breach parameters. J. Hydraul. Eng. ASCE 5, 389–397.
Walder, J.S., O'Connor, J.E., 1997. Methods for predicting peak discharge of floods caused by failure of natural and constructed earthen dams. Water Resour. Res. 33, 2337–2348.
Walder, J.S., Costa, J.E., 1996. Outburst floods from glacier-dammed lakes: The effect of mode of lake drainage on flood magnitude. Earth Surf. Process. Landf. 21, 701–723.
Walder, J.S., Driedger, C.L., 1994. Rapid geomorphic change caused by Glacial Lake Outburst Floods and debris flows along Tahoma Creek, Mount Rainier, Washington, U.S.A. Arct. Alp. Res. 26, 319–327.
Walder, J.S., Watts, P., Sorensen, O.E., Janssen, K., 2003. Tsunamis generated by subaerial mass flows. J. Geophys. Res. 108. http://dx.doi.org/10.1029/2001JB000707.
Wan, C.F., Fell, R., 2004. Investigation of rate of erosion of soils in embankment dams. J. Geotech. Geoenviron. Eng. ASCE 130, 373–380.
Watanabe, T., Kameyama, S., Sato, T., 1995. Imja Glacier dead-ice melt rates and changes in a supra-glacial lake, 1989–1994, Khumbu Himal, Nepal: danger of lake drainage. Mt. Res. Dev. 15, 293–300.
Watanabe, T., Rothacher, D., 1994. The 1994 Lugge Tsho Glacial Lake Outburst Flood, Bhutan Himalaya. Mt. Res. Dev. 16, 77–81.
Wessels, R.L., Kargel, J.S., Kieffer, H.H., 2002. ASTER measurement of supraglacial lakes in the Mount Everest region of the Himalaya. Ann. Glaciol. 34, 399–408.
Westoby, M.J., Brasington, J., Glasser, N.F., Hambrey, M.J., Reynolds, J.M., 2012. 'Structure-from-Motion' photogrammetry: a low-cost, effective tool for geoscience applications. Geomorphology 179, 300–314.
Whetmore, J.N., Fread, D.L., Lewis, J.M., Wiele, S.M., 1991. The NWS Simplified Dam-break Flood Forecasting Model. Hydrologic Research Laboratory, National Weather Service, Silver Spring, Md (47 pp.).
Wetmore, J.N., Fread, D.L., 1984. The NWS Simplified Dam-Break Flood Forecasting Model. Hydrologic Research Laboratory, Office of Hydrology, NWS, NOAA.
Wohl, E.E., 1998. Uncertainty in flood estimates associated with roughness coefficient. J. Hydraul. Eng. ASCE 124, 219–223.
Williams, G.P., 1978. Bank-full discharge of rivers. Water Resour. Res. 14, 1141–1154.
Williams, G.P., 1984. Paleohydraulic equations for rivers. In: Costa, J.E., Fleisher, P.J. (Eds.), Developments and Applications of Geomorphology. Springer, Berlin, pp. 343–367.
Worni, R., Stoffel, M., Huggel, C., Volz, C., Casteller, A., Luckman, B., 2012. Analysis and dynamic modelling of a moraine failure and glacier lake outburst flood at Ventisquero Negro, Patagonian Andes (Argentina). J. Hydrol. http://dx.doi.org/10.1016/j.jhydrol.2012.04.013.
Xu, Y., Zhang, L.M., 2009. Breaching parameters for earth and rockfill dams. J. Geotech. Geoenviron. Eng. ASCE. http://dx.doi.org/10.1061/(ASCE)GT.1943-5606.0000162.
Xia, J., Lin, B., Falconer, R.A., Wang, G., 2010. Modelling dam-break flows over mobile beds using a 2D coupled approach. Adv. Water Resour. 33, 171–183.
Xin, W., Shlyln, L., Wanqin, G., Junll, X., 2008. Assessment and simulation of Glacier Lake Outburst Floods for Longbasaba and Pida Lakes, China. Mt. Res. Dev. 28, 310–317.
Xu, Q., Shang, Y.J., van Asch, T., Wang, S.T., Zhang, Z.Y., Dong, X.J., 2012. Observations from the large, rapid Yigong rock slide-debris avalanche, southeast Tibet. Can. Geotech. J. 49, 589–606.
Yamada, T., 1998. Glacier Lake and its Outburst Flood in the Nepal Himalaya. Monograph No. 1 Data Center for Glacier Research, Japanese Society of Snow and Ice, Tokyo (11 pp.).
Yao, X., Liu, S., Sun, M., Wei, J., Guo, W., 2012. Volume calculation and analysis of the changes in moraine-dammed lakes in the north Himalaya: a case study of Longbasaba lake. J. Glaciol. 58, 753–800.
Zhang, S., Duan, J.G., 2011. 1D finite volume model of unsteady flow over mobile bed. J. Hydrol. 405, 57–68.